
DIGITAL ACCESS TO SCHOLARSHIP AT HARVARD
DASH.HARVARD.EDU

HARVARD LIBRARY


Determining Synthetic Lethal Targets in DNA Polymerase Epsilon P286R Mutants Using Genome-wide CRISPR-Cas9 Knockout Screens

Citation

Doiron-LaRue, Ethan Emile. 2022. Determining Synthetic Lethal Targets in DNA Polymerase Epsilon P286R Mutants Using Genome-wide CRISPR-Cas9 Knockout Screens. Master's thesis, Harvard University Division of Continuing Education.

Link

https://nrs.harvard.edu/URN-3:HUL.INSTREPOS:37371699

Terms of use

This article was downloaded from Harvard University's DASH repository, and is made available under the terms and conditions applicable to Other Posted Material (LAA), as set forth at

https://harvardwiki.atlassian.net/wiki/external/NGY5NDE4ZjgzNTc5NDQzMGIzZWZhMGFlOWI2M2EwYTg

Accessibility

https://accessibility.huit.harvard.edu/digital-accessibility-policy

Share Your Story

The Harvard community has made this article openly available.
Please share how this access benefits you. Submit a story

Determining Synthetic Lethal Targets in DNA Polymerase Epsilon P286R Mutants Using Genome-wide CRISPR-Cas9 Knockout Screens

Ethan Doiron-LaRue

A Thesis in the Field of Biology

for the Degree of Master of Liberal Arts in Extension Studies

Harvard University

May 2022

Copyright 2022 Ethan Doiron-LaRue

Abstract

Genomic instability is an important hallmark of cancer development and is often a product of impaired or abnormal DNA replication. For instance, DNA Polymerase Epsilon (POLE) is responsible for the bulk of DNA replication on the leading strand, and somatic mutations mapping to the 'proof-reading' exonuclease domain, such as *POLE*$^{P286R/+}$, are commonly detected in tumors of the endometrium and gastrointestinal tract. *POLE* exonuclease domain mutations are frequently associated with increased mutational burden and can be further sub-classified as either 'microsatellite stable' (MSS) or 'instable' (MSI), depending on the functionality of compensatory mismatch repair (MMR) pathways. Genetic dependencies in MSS cancers bearing *POLE* mutations are poorly understood, however, previous studies modeling analogous mutations in yeast demonstrated increased levels of replication stress irrespective of MMR status. We therefore predicted that human MSS *POLE* mutant cancer cells would show enhanced sensitivity to pharmacologic inhibition of ATR, the master-regulator of replication fork stability. Furthermore, our i*n-silico* predictions indicate that DNA damage repair (DDR) genes downstream of ATR, including *FANCM*, *MSH2*, and *MSH6*, are more heavily relied upon in patient-derived MSS *POLE* mutant cancer cell lines relative to those without *POLE* mutations. Towards this end, we used CAS9 to create human *U2OS*-derived *POLE*$^{P286R/+}$ knock-in cell lines. Indeed, we observed distinct replication fork abnormalities and reduced viability in the presence of ATRi in *POLE*$^{P286R/+}$ cells relative to isogenic controls.

To validate our *in-silico* predictions and to identify additional synthetic-lethal targets *in-vitro*, we designed a custom CRISPR knockout (KO) library with particular emphasis on genes known to be involved in DNA replication and repair, including ample representation of targets previously implicated in ATR-dependent signaling pathways. We further engineered and optimized our *POLE* isogenic cell line pairs to enable doxycycline-inducible expression of CAS9 following introduction of the KO library. The results of our pilot screen are currently pending next-generation sequencing and analysis. Future works will be focused on putative target validation and additional mechanistic inquiry, the summation of which will provide important insight towards the development of novel therapies capable of selectively killing MSS *POLE* mutant cancers.

Dedication

I would like to firstly dedicate this work to the millions of those who perished from the terrible COVID-19 pandemic that's currently tearing through the world, as well as the professionals that are doing their best to keep the rest of humanity from meeting the same fate. Those who are surviving through this harsh and unforgiving disease will have their lives forever changed by the mark this virus has left, and that goes doubly so for the medical professionals on the forefront of this catastrophe. The scars that his pandemic will leave, whether they be mental or physical, will stay with the survivors like a grief. These scars may heal with time, but what the virus has taken from the world can never be given back, and for some the virus took all they had to be taken. As COVID-19 reaches its third year since discovery, it is my hope that humanity reaches a point where ignorance and fear no longer holds us back from slowing or preventing this disease and we can begin to tend to our grief.

Secondly and on a much warmer note, I'd also like to dedicate this work to my fiancé Emily, who made this work possible by giving me a place to shelter from the harsh months through which it was worked on. Her caring and compassion during the difficult times while this thesis was being crafted was a harbor in a storm, and I'm not sure how I would've made it through these perilous times without her company. I thank her from the bottom of my heart and can't imagine this work being done without her, since I can't imagine myself in any aspect without her either.

Acknowledgments

I would like to acknowledge my thesis director Dr. Jessica Hopkins, who has made this thesis project possible. While we may stand on the shoulders of giants, I certainly stood very heavily on the shoulders of this giant in particular, and her assistance in technique, theory, and project development has been absolutely critical to the progress of both myself and this project. Her patience while guiding me through the process has been very much appreciated, and her guidance has helped me make my time at MGH as impactful as possible. Dr. Antoine Simoneau's advisement has also played a role in experiment development, and so I truly appreciate all the time, code, and reagents that he graciously donated to my cause. I also thank Dr. Sneha Saxena, who assisted in the preparation of this thesis, and Dr. Jian Ouyang, who provided important training and feedback during my tenure at MGH.

I would also like to acknowledge the Zou, Dyson, and Lawrence labs at MGH. The intellect, fraternity, and overall enthusiasm to work as a team is difficult to find at a level that it is present in that lab, and exposure to such an environment during my time there has given me a newfound appreciation for academic researchers. The work being performed there is truly breathtaking, and it gives me hope for future cancer patients that a team of excellent researchers like the ones working in the Zou lab are working to find key players in DNA damage repair and finding ways to target them in cancer.

Table of Contents

Dedication vi

Acknowledgments vii

List of Tables xi

List of Figures xii

Chapter I. Introduction 1

DNA Polymerase 1

Function 1

Mutations and Pol-Dependent Tumorigenesis 2

Genetics of Mutations. 3

Tissues Known to Develop Pol-related Tumors. 6

Functional Drivers of Tumorigenesis. 7

Signatures of Pol Mutations. 8

Mismatch Repair in the Context of Pol Mutations. 11

Indications and Targeting of Genetic Dependencies in MSS *POLE*-Mutant Tumors 14

The Mismatch Repair Pathway 17

Fanconi Anemia Genes. 18

ATR in Replication and DNA Damage Response 19

The Role of ATR in the MMR Pathway 20

The Role of ATR in the FA Pathway 21

Modeling *POLE* Mutations....21
Generating Knock-in Mutations Using Cas9....23
CRISPR-Cas9 Knockout Screening....23
Research Aims, Goals, and Hypothesis....25
Chapter II. Materials and Methods....27
$POLE^{P286R/+}$ Mutant Generation....27
Confirmation of Phenotype....33
Transduction and Functionality Screening of Inducible Cas9....34
DNA Fiber Assay....40
DNA Damage Response Focused CRISPR-Cas9 Knockout Screen....42
Chapter III. Results....45
Viability Assay....45
DNA Fiber Assay....46
Chapter IV. Discussion....49
Significance of Results....49
Genetic Dependencies Generated from Cancer Dependency Databases....52
Study Limitations....59
Future Research Directions....60
Treatment Options for Genetic Dependencies....61
Conclusion....67
Appendix 1. Genes Targeted by KO Library....68
gRNA and ssODN Sequences for $POLE^{P286R}$ Knock-in....80
Additional Fiber Assay Results....81

References.....83

List of Tables

Table 1. Representative Cell Lines and Their Genetic Dependencies.....54

Table 2. Genes Targeted by KO Library.....80

List of Figures

Figure 1. Function of DNA Polymerases and Their Domains 2

Figure 2. Frequency of *POLE* and *POLD1* Mutations Based on Tumor Types 5

Figure 3. Mutation Types and Locations Along *POLE* and *POLD1* Genes 6

Figure 4. Microsatellite Status and DNA Polymerase Mutation.....13

Figure 5. Genetic Dependencies of *POLE*-mutated MSS Cell Lines vs. non *POLE*-mutated MSS Cell Lines 16

Figure 6. Recruitment and Function of Mismatch Repair Proteins.....17

Figure 7. Workflow of Thesis 25

Figure 8. Inducible Cas9 Expression in Isogenic Controls and $POLE^{P286R/+}$ Cells...38

Figure 9. Cas9 Effectiveness in Targeting Critical Gene *RPS19* 40

Figure 10. Cas9 Expression During KO Screen.....43

Figure 11. Viability Assay.....46

Figure 12. DNA Fiber Assay.....48

Figure 13. Cell Line Sensitivities to ATR Inhibitors 56

Figure 14. Average DMSO Treated Fiber Length 81

Figure 15. Additional Fiber Assay Results 82

Chapter I.

Introduction

DNA Polymerase

Function

Human cells utilize three DNA polymerases (Pols) for nuclear DNA replication during cellular division; Polymerase α, δ, and ε. DNA Pol α initiates each DNA synthesis reaction after the primase subunit has added a primer of 8-12 RNA nucleotides to the template, after which Pol α elongates the primers for roughly 20 nucleotides (Garg & Burgers, 2005). The process of replication is then taken over by DNA Pols δ (*POLD1*) and Pol ε (*POLE*) to complete the bulk of replication, whereby Pol ε synthesizes the leading strand and the Pol δ synthesizes the lagging strand. These polymerases consist of multiple subcomponents, both being formed by heterotetramers of four subunits (Jain et al., 2018). In each of these heterotetramers there is a single protein subunit that contains a polymerase domain, which is the catalytic active site responsible for synthesis, and a "proofreading" exonuclease domain, responsible for recognizing and removing misincorporated nucleotides during synthesis. The polymerase domain is highly selective, only making approximately one misinsertion every 10^5 nucleotides synthesized, while the exonuclease domain acts to detect mismatch incorporation into the synthesized DNA, increasing the accuracy of the polymerase by 10- to 100- fold (Kunkel, 2009). The polymerase and exonuclease domain are thus thought to compete for DNA substrate, with the exonuclease domain having an inhibitory effect on the polymerase domain, slowing the process of DNA

synthesis while mismatched nucleotides are recognized and removed (Xing et al., 2019). These domains, along with mismatch repair (MMR) processes that follow up the synthesizing of DNA, allow for high fidelity replication and a low mutational load in healthy cells (Figure 1).

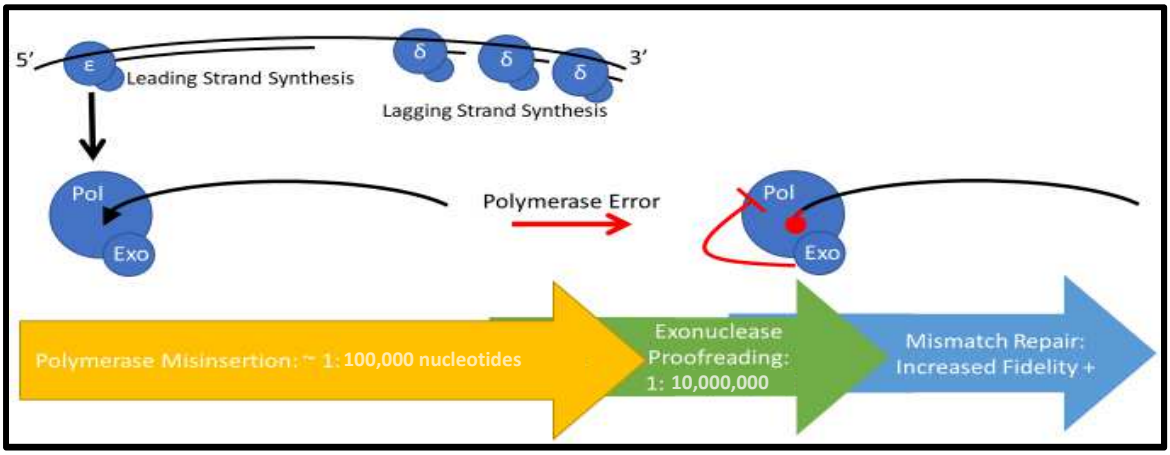


Figure 1. Function of DNA Polymerases and Their Domains

Polymerase ε synthesizes DNA on the leading strand while Polymerase δ synthesizes on the lagging strand. As the POL domain functions to replicate the template strand, the EXO domain functions to "proofread" the nucleotides as they're being synthesized. If an error is detected, the EXO domain inhibits DNA synthesis and excises the mismatch. Below, arrows indicate the fidelity of replication based on the polymerase, exonuclease, and mismatch repair's role (Kunkel, 2009; Xing et al., 2019).

Mutations and Pol-Dependent Tumorigenesis

As *POLE* and *POLD1* are the genes responsible for the accurate duplication of the genome during replication, it follows that cancers, experiencing positive selection for high mutational rates and unstable genomes, will arise with aberrations in these genes (Martincorena & Campbell, 2015). This section will discuss the genetics, affected tissues,

signatures, secondary mutations, and the MMR pathway in relationship to *POL* mutations to the aim of clarifying the difference between early and late-stage cancers stemming from these mutations.

Genetics of Mutations. Mutations in *POLE* and *POLD1* often lead to an increase in the mutational burden in cells during replication (Robinson et al., 2021). Mutations in these genes are most common in endometrial, gastrointestinal, and colon cancers, but are also seen in brain, pancreatic, and skin cancers (Figure 2). Mutations in the *Pol* genes primarily occur in regions coding for the exonuclease or the catalytic domains of the polymerases. While *POLE* mutations predominantly affect the exonuclease domain, *POLD1* mutations are spread relatively equally across the domains (Figure 3). The most commonly observed types of mutations in these genes are substitution mutations, with many variants seen in each of the *Pol* genes. For *POLE*, the most common mutations are P286R and V411L, making up a vast majority of the mutations seen in cancers (Rayner et al., 2016). In *POLD1*, the substitution mutations are much more varied, but the S478N mutation is the most common. However, there are many other substitution mutations in both genes that confer a proofreading defect, with novel variants still being discovered and validated as pathogenic. Indeed, Esteban-Jurado et al. show that clinical features indicative of polymerase proofreading defects, such as multiple polyps or early onset colorectal cancer (CRC), were not predictive of the presence of well-characterized *POL* hotspot mutations in a cohort of 155 patients (Esteban-Jurado et al., 2017). This growing diversity of uncharacterized *POL* mutations necessitates further validation of pathogenicity. This is often done by estimating the apparent mutation rate associated with the expression of the mutated *POL* allele in mouse and yeast models. Yeast are particularly well-suited as a

model system due to DNA replication being fairly conserved across eukaryotes, as well as yeast having homologs to *POLE* and *POLD1* (Burgers & Kunkel, 2017; Kesti et al., 1999). Mutations in different POL domains confer unique changes leading to pathogenicity. For example, *POLD1-R696W*, a mutation commonly seen in the exonuclease domain of *POLD1* in CRC, causes infidelity in nucleotide selection which causes a downstream increase in dNTP pools when modeled in yeast, thereby increasing infidelity and causing a vicious cycle of mutation accumulation and genomic instability (Mertz et al., 2015). $POLE^{P286R}$, the hotspot exonuclease domain mutation most commonly seen in sporadic cancers, impedes the proofreading function of the protein while simultaneously increasing the activity of the polymerase domain when modeled in yeast (Xing et al., 2019). This phenomenon is thought to occur due increased substrate binding in the competing polymerase domain.

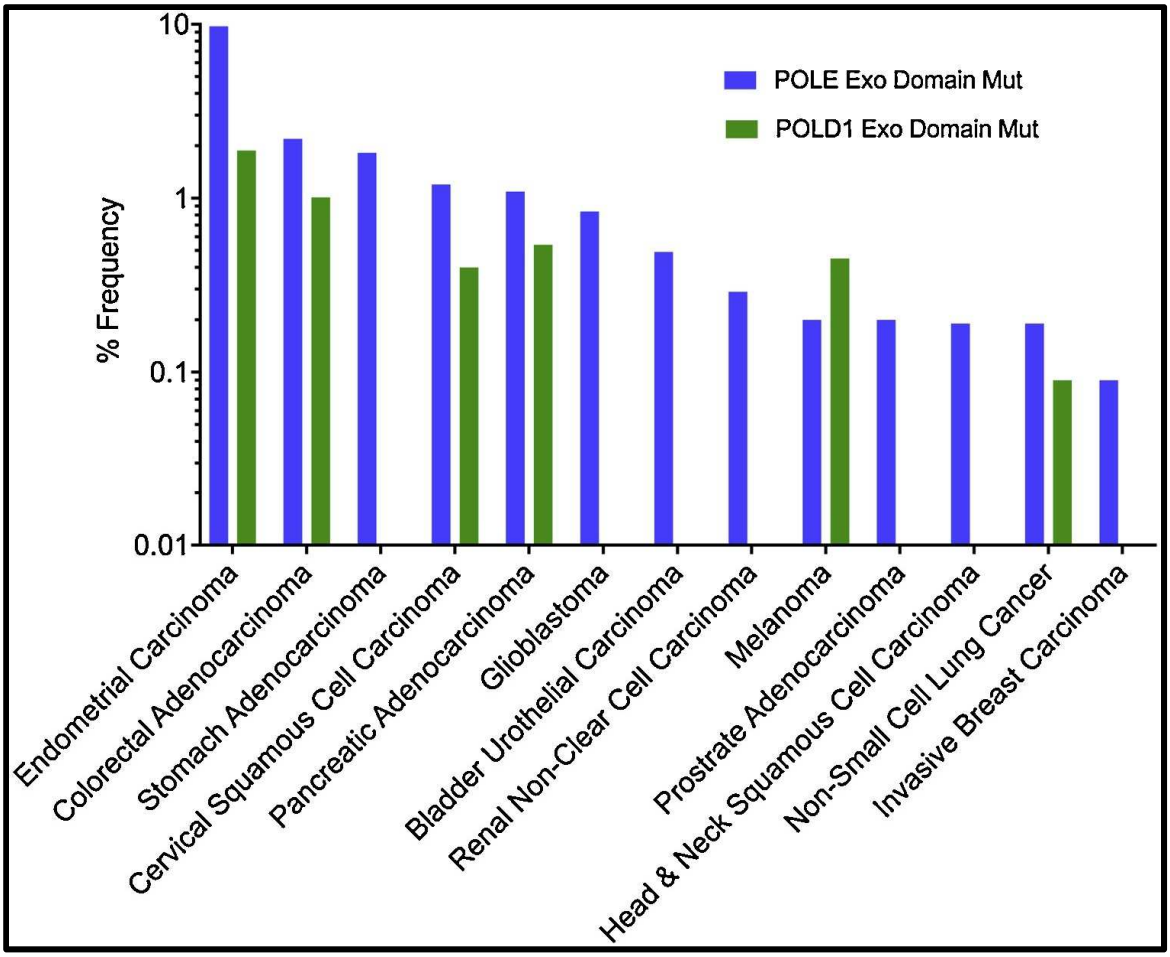


Figure 2. Frequency of *POLE* and *POLD1* Mutations Based on Tumor Types

Endometrial carcinoma is the tumor in which POLE *is roughly 10-fold more likely to be mutated when compared to other cancer types with polymerase mutations, but mutations in both* POLD1 *and* POLE *are seen with a lower frequency in many tissue types (Park & Pursell, 2019).*

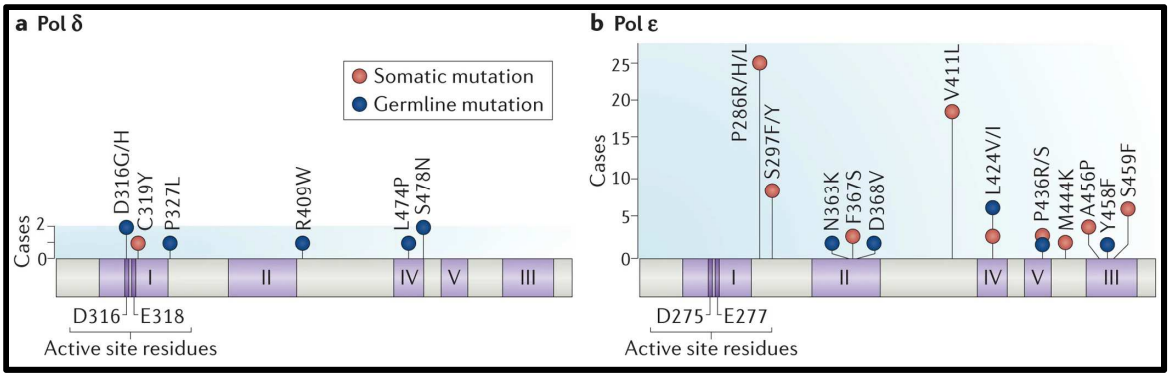


Figure 3. Mutation Types and Locations Along *POLE* and *POLD1* Genes

Rayner et al. summarize exome sequencing of 224 sporadic CRC tumors by The Cancer Genome Atlas. The sequencing revealed the various substitution mutations and locations along the POLD1 *and* POLE *genes, with S478N being the most common mutation in* POLD1 *and P286R/H/L and V411L being close in frequency as the most common mutation in* POLE. *(Rayner et al., 2016)*

Tissues Known to Develop Pol-related Tumors. As previously mentioned, *POL* mutations are most common in CRC and endometrial cancers (EC), but there are many different tissues in which the *POL* mutations are seen to drive tumorigenesis. The syndrome in which inherited germline or somatic mutations in the proofreading domain of these polymerases cause precancerous polyps to form in the endometrium and the gastrointestinal tract has been classified as Polymerase Proofreading-Associated Polyposis (PPAP), and the involvement of these mutations in carcinogenesis in various tissues is still being determined (Briggs & Tomlinson, 2013). Predictably, patients with PPAP developed CRC most frequently, with EC being the second most frequently developed cancer. In a follow-up study, PPAP patients were also seen developing breast, duodenal, and brain tumors, with varying frequency of tumorigenesis in the tissue, depending on the mutated *POL* (Palles et al., 2021). There are also inherited mutations in the MMR pathway dubbed

biallelic MMR deficiency (bMMRD), in which secondary mutations in *POL* genes are typically seen at an early age, resulting in hypermutated brain tumors that have rates of mutational burden rarely seen in adult tumors (Shlien et al., 2015). This variation of tissues in which tumors are found in the presence of germline or somatic *POL* mutations indicates that there are multiple mechanisms by which *POL* mutant tumors can arise and sparks the debate on whether *POL* exonuclease domain mutations function to drive tumorigenesis or are passenger mutations that function to speed the mutational burden of these cells.

Functional Drivers of Tumorigenesis. As there are a wide range of *POL* mutations that are seen in tumors, there has been uncertainty regarding which, if any, mutations are sufficient to be "driver" mutations which act to cause downstream mutations that cause tumorigenesis, and which are simply "passenger" mutations that develop subsequently. Investigation of patient-derived tumors show that even when tumors with novel and uncharacterized *POL* mutations have many of the hallmark indicators of pathogenic *POL* mutations such as early-onset CRC or multiple polyps, many of the *POL* mutations don't show defects indicative of pathogenic polymerase activity. This suggests that mutations in *POL* may not be the primary mechanism by which tumors arise and may therefore be passenger mutations (Esteban-Jurado et al., 2017). Multiple other genes have been shown to be functional as driver mutations in CRC, such as MMR genes *MSH3* and *MSH6*, cell signaling genes such as *KRAS*, and cell cycle regulators such as *TP53* (Carethers & Jung, 2015). These driver mutations promote genomic instability that may lead to mutations in secondary genes such as *POLE* without depending on that gene for tumorigenesis. Hence, a mutation in a *POL* gene might not always be indicative of a Pol-dependent tumor (Tomasetti et al., 2015; Vogelstein et al., 2013). However, as research continues, it is

increasingly evident that there are multiple *POL* mutations that can indeed drive tumorigenesis, including the commonly seen heterozygous $POLE^{P286R/+}$ missense mutation (Temko et al., 2018). The fact that these mutations are seen in non-malignant precursors of EC and CRC, as well as the mutational signatures seen in the cancers of other patients, indicates that they are likely the driving factor of these precancers. In mouse models, $POLE^{P286R/+}$ has been shown to be sufficient for downstream mutation or inactivation of *TP53*, a gene regarded as a hurdle for *POL* mutations to drive tumorigenesis. This study also found that most $POLE^{P286R/+}$ tumors do not spontaneously undergo mutations in *MSH2* and cooperate with defective MMR in tumor progression. (Li et al., 2020). There is also evidence that *POLE* driver mutations in the exonuclease domain exhibit a specific clinical pattern, with distinct *POLE* mutations driving the enrichment of specific *TP53* mutations in Pol ε-driven CRCs (Fang et al., 2020; Hu et al., 2021). This suggests that $POLE^{P286R/+}$ or another heterozygous *POLE* exonuclease domain mutation alone can result in Pol ε-driven mutations resulting in cancer.

Signatures of Pol Mutations. Tumors are usually characterized as being Pol-dependent or Pol-related by genotyping (Palles et al., 2021). Tumors driven by *POL* mutations are hypermutated, although mutagens such as UV-light and carcinogens present in tobacco smoke may also cause hypermutation, and so factors such as tumor location and mutational signatures must be considered (Campbell et al., 2017). COSMIC, the Catalog Of Somatic Mutations In Cancer, has been compiling signatures of various sources of mutations and has been a boon to researchers and medical professionals who have been using it to classify tumors (Tate et al., 2019). There are three known mutational signature categories that are

being tracked by COSMIC: Single Base Substitutions (SBS), Double Base Substitutions (DBS), and Insertions or Deletions (ID). To quote COSMIC:

> SBS, also known as single nucleotide variants, are defined as a replacement of a certain nucleotide base. Considering the pyrimidines of the Watson-Crick base pairs, there are only six different possible substitutions: C>A, C>G, C>T, T>A, T>C, and T>G. These SBS classes can be further expanded considering the nucleotide context.
>
> Current SBS signatures have been identified using 96 different contexts, considering not only the mutated base, but also the bases immediately 5' and 3'.
>
> DBS are generated after the concurrent modification of two consecutive nucleotide bases. There are 78 strand-agnostic DBS mutation types, enumerated here.
>
> More specifically, there are 16 possible source doublet bases (4 x 4). Of these, AT, TA, CG, and GC are their own reverse complement. The remaining 12 can be represented as 6 possible strand-agnostic doublets. Thus, there are 4+6=10 source doublet bases. Because they are their own reverse complements, AT, TA, CG, and GC can each be substituted by only 6 doublets. For the remaining doublets, there are 9 possible DBS mutation types (3 x 3). Therefore, in total there are 4 x 6 + 6 x 9 = 78 strand -agnostic DBS mutation types.
>
> ID [insertions or deletions], also known as indels, are defined as the incorporation or loss of small fragments of DNA (usually between 1 and 50 base pairs) in a specific genomic location.
>
> Although there is no single intuitive and naturally constrained set of ID mutation types (as there arguably are for single base substitutions and doublet base substitutions), a compilation of 83 different types considering size, nucleotides affected and presence on repetitive and/or microhomology regions was used to extract mutational signatures.

These mutational signatures are based on the genomic insult that results in tumorigenesis. For instance, tobacco smoke generates all three types of signatures and hence is seen in all three mutational signature categories (Alexandrov et al., 2016). The identification of these mutational signatures is impactful since they allows researchers to identify a "fingerprint" of the mutagenic process on the genome, and may reflect a genetic dependency that is

consistent in cell lines or tumors that have these signatures (Ma et al., 2018). Cells with deficiency in the homologous repair (HR) pathway have been identified to have the COSMIC signature SBS3, which is strongly associated with *BRCA1* and *BRCA2* mutations or silencing by methylation (Zámborszky et al., 2017). Cancers deficient in the HR pathway have also been discovered to have genetic dependencies in other DNA Damage Repair (DDR) pathways in order to compensate for the loss of HR. These genetic dependencies have proven to be excellent targets for therapeutic agents in the course of cancer treatment, for instance, the inhibition of PARP, which is involved in the repair of single-strand breaks in DNA (Mateo et al., 2015). This genetic dependency based on a mutation that results in a specific COSMIC signature can be theoretically applied to other COSMIC signatures, offering interesting avenues for testing and treatment.

POL mutations also give rise to specific mutational signatures, and those signatures can vary based on the mutation (Hu et al., 2021). Since the field of mutational signatures is still developing, there are many signatures that have been consistently found in tumors but have yet to be classified under a specific etiology. Recent research suggests that ID10, one of the unclassified mutational signatures, may be associated with a *POLE* exonuclease mutation, indicating that there may be more mutational signatures dependent on *POLE* yet to be discovered (Fang et al., 2020). There are also other mutational signatures that have been proposed to be associated with *POL* mutations, such as SBS10, SBS14, SBS20, and DBS3 (Alexandrov et al., 2020). This indicates that specific mutations of either *POLD1* or *POLE* are more likely to have recurrent erroneous incorporation of nucleotides as it replicates DNA, and these recurrent errors allow the genotyped tumor to be identified as driven by a *POL* mutation. This mutational signature is how *POL* mutations were

identified as drivers of tumorigenesis and also gives insights on how *TP53* was determined to be mutated by dysfunctional Pol ε (Fang et al., 2020; Hu et al., 2021). These mutational signatures that are recurrent in cancers with *POL* mutations also raise the possibility that these cancers may rely on specific DDR genes to compensate for this deficiency in replication. Using the same logic as that applies to HR deficient cells, the investigation of a synthetic lethal target that *POL* mutants depend on is an attractive avenue for research. Indeed, researchers have linked ATR and *POLD1* as synthetic lethal knockouts in the human CRC cell line DLD1, and while these experiments don't replicate exonuclease domain mutations that are more commonly seen in CRCs, they do broach the topic of synthetic lethal targets in Pol-deficient cancers (Hocke et al., 2016). This will be discussed at length in the 'Indications of Genetic Dependencies in MSS *POLE* Mutant Tumors' section of this thesis

Oftentimes, cancers with mutations in *POL* will develop a secondary mutation in the MMR pathway, and there are multiple mutational signatures associated with both the MMR pathway alone as well as *POL* and MMR pathway mutations combined, intertwining the two in mutational signatures and cancer development (Alexandrov et al., 2020). As described in the previous section, there is uncertainty of which mutation is driving the tumorigenesis in such cancers. While recent studies suggest that a *POL* mutation can drive the MMR pathway to become secondarily mutated or silenced, the polymerase proofreading and mismatch repair processes are often concurrently lost in cancers (Haradhvala et al., 2018).

Mismatch Repair in the Context of Pol Mutations. As introduced previously, there is also an additional method to identify mutations in the MMR pathway beyond COSMIC

signatures. Mutations in the MMR pathway also lead to additional genomic insults in areas of short, tandemly repeated sequences that are present throughout the genome (B. Liu et al., 1995). These repeated sequences known as microsatellites, are erroneously repaired by the MMR pathway (Kawakami et al., 2015). Cells with mutations in the microsatellite regions of the genome, by means of small insertions or deletions, are referred to as having microsatellite instability (MSI), which is known to indicate inefficient MMR (Boland & Goel, 2010). In contrast, microsatellite stable (MSS) cells lack such mutations in microsatellite regions of their genomes, indicating a functioning MMR pathway, but can still acquire a high mutational burden by Pols with erroneous proofreading (Bourdais et al., 2017).

Tumors that have mutations in *POLE* co-occur with both MSI and MSS, while *POLD1* mutant tumors are only found in MSI contexts (Figure 4) (Park & Pursell, 2019). This could be due to Pol δ having a role in the MMR itself, with studies implicating that mutations in the *POLD1* reduce the efficiency of MMR (D. Liu et al., 2017). However, MMR deficiency is still heavily indicated as a secondary factor in these polymerase mutant tumors, as suppression of MMR in $POLE^{P286R}$ mutant cells leads to severe mutational loads in the genome and leads to MSI tumors (Hodel et al., 2018).

An important distinction must be drawn between MSS and MSI tumors, as they not only have different mutational signatures, but exhibit different responses to treatment as well (Markowitz et al., 1995). There may be a close relationship between Pol and MMR mutations, but the tumors that arise from one, the other, or a combination of the two must be recognized as different entities with different mutational landscapes.

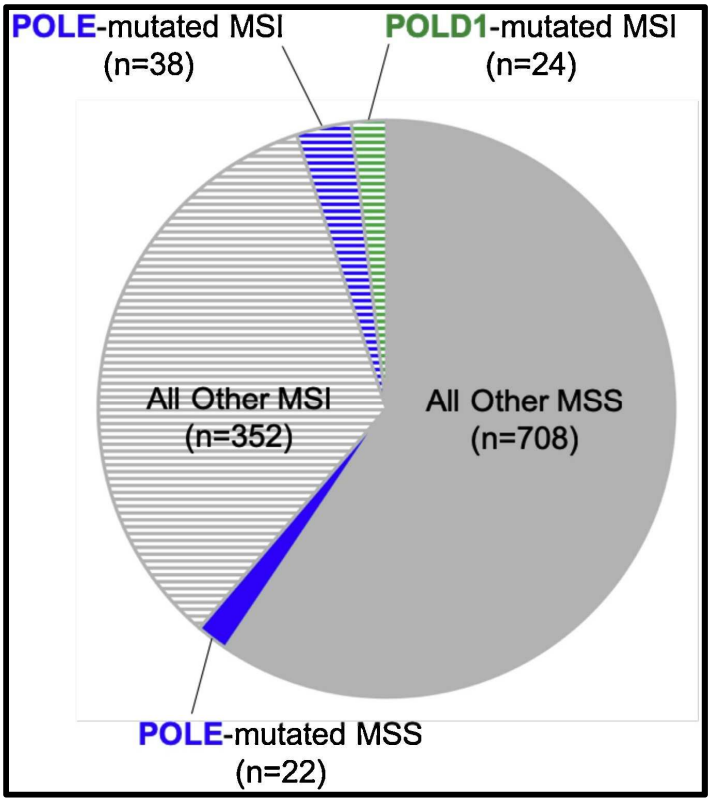


Figure 4. Microsatellite Status and DNA Polymerase Mutation

Analyzing 5 studies with 8,000 discrete tumors, Park and Pursell found 1,144 tumors with their microsatellite status and whole exome/genome sequence reported. Among these, 3% of MSS and 10% of MSI tumors were found to have POLE *mutations while 6% of MSI tumors were found to have* POLD1 *mutations. There were no MSS tumors found to have* POLD1 *mutations. (Park & Pursell, 2019)*

To summarize, mutations in the exonuclease domain of *POLD1* and *POLE* genes cause proofreading defects, leading to the development of cancer in the colon and endometrium, among other tissues (Briggs & Tomlinson, 2013; Palles et al., 2021). These proofreading-defect mutations alone have been found to drive tumorigenesis by mutating or otherwise silencing other DDR pathways, including MMR (Fang et al., 2020; Hu et al., 2021; Li et al., 2020; Temko et al., 2018). Deficiencies in the MMR pathway are indicated

by MSI, and while many tumors with *POL* mutations are found to have MSI, some *POLE*-mutant tumors are found to be MSS, indicating that heterozygous *POLE*-mutant tumors can develop separately from MMR silencing (Park & Pursell, 2019). This can be confirmed by mutational signatures created by exonuclease-deficient Pol ε that are also discrete from MMR deficiencies. Previous work focusing on other mutational signatures suggest methods to identify mutations that are promoting tumorigenesis based on the mutational signature, along with targetable genetic dependencies that are associated with those signatures (Alexandrov et al., 2020; Ma et al., 2018; Mateo et al., 2015). There are also studies indicating that $POLE^{P286R}$ mutations early in tumor development may increase the mutational burden of the cell prior to transformation and that these cells may rely on the MMR pathway to keep the mutational burden sustainable in this early timeframe in tumor development (Hodel et al., 2018). This indicates a unique dependence on the MMR pathway in both early and late-stage tumors deficient in Pol ε proofreading, which may be used to target such tumors by disrupting the MMR pathway directly or by targeting key components in a related DDR pathway such as ATR. With these findings in mind, we will be focusing our research on the genetic dependencies in cells with the most commonly seen *POLE* mutation $POLE^{P286R}$, which has been identified as pathogenic and associated with MSS contexts in patients, as well as verified to be hypermutational (>10 mutations/Mb) in *S. cerevisiae* (Barbari et al., 2018; Rayner et al., 2016).

Indications and Targeting of Genetic Dependencies in MSS *POLE*-Mutant Tumors

In the context of cancer, mutations in *POLE* often precede a secondary mutation in the MMR pathway that causes MSI (Haradhvala et al., 2018). However, there are also many cases in which there is a mutation in *POLE* where the tumor is noted to be MSS and

has functioning MMR. Also, to reiterate what has been touched on previously, tumors that have defects in the MMR pathway with simultaneous *POL* mutations have a different mutational landscape when compared to a tumor with deficiencies in only one of the two, and these tumors therefore have different genetic dependencies and respond differently to treatments (Alexandrov et al., 2020; Fang et al., 2020). Indeed, research from collaborators investigating genetic dependency databases indicate that tumors that are MSS but that also have mutations in *POLE* have a differing reliance on genes when compared to MSS tumors that don't have a mutation in *POLE* (Figure 5). The genes that are heavily relied upon in this study are within the MMR pathway, seen as a reliance on *MSH6* and *MSH2* genes, as well as the Fanconi Anemia (FA) pathway, as seen in a reliance on the *FANCM* gene. This work by our collaborators in the Mike Lawrence lab is what leads us to hypothesize that there exist genetic dependencies present in *POLE* mutants that are not found in cells that do not have a *POLE* mutation, and also gives us an insight into what pathways those dependencies might fall into.

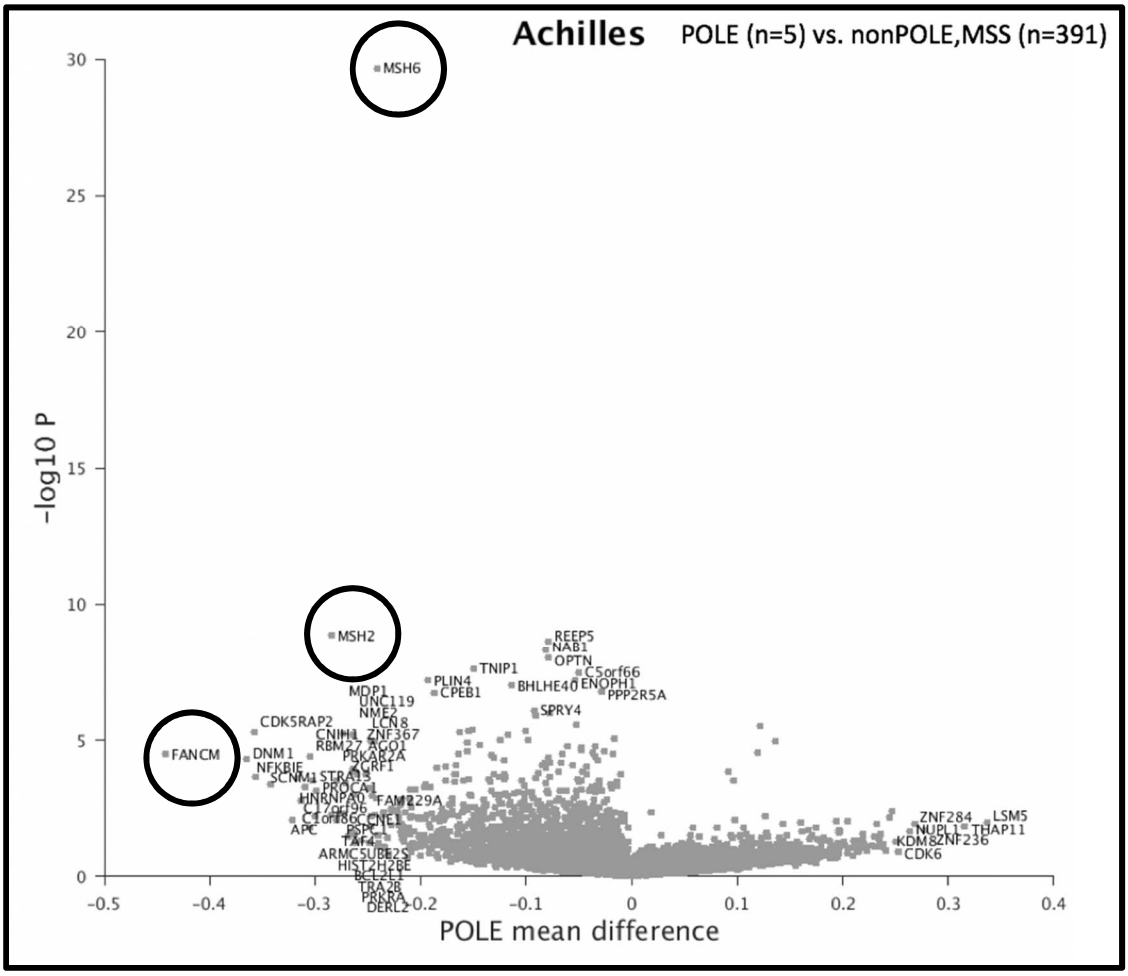


Figure 5. Genetic Dependencies of *POLE*-mutated MSS Cell Lines vs. non *POLE*-mutated MSS Cell Lines

Our collaborators in the Mike Lawrence lab used known cell lines with genetic dependencies found on DepMap to create a volcano plot showing the genetic dependencies on genes in POLE-*mutated MSS cell lines when compared to non*POLE-*mutated MSS cell lines. The y-value indicates the significance of the dependency while the x-value indicates the mean difference in the comparison between the two groups. MMR genes MSH2 and MSH6, as well as FA gene FANCM are among the most likely dependencies.*

The Mismatch Repair Pathway

MMR pathway genes are among the most common secondary mutations in *POLE* mutation-driven CRCs. This would imply that tumors with mutations in other DDR pathways that allow for genetic instability would rely heavily on MMR to limit the mutational burden. MMR functions by recognizing, excising, and correcting mismatches on daughter strands (Li, 2008). MutS Homolog 2 (MSH2) heterodimerizes with either MSH3 or MSH6 to form MutS, and this heterodimer functions to recognize the mismatching nucleotides and initiate mismatch repair. MutL Homolog 1 (MLH1) heterodimerizes with PMS1, PMS2, or MLH3, forming a heterodimer known as MutL that interacts with MutS to regulate the excision of mismatched nucleotides, and also regulates DNA replication on the daughter strand that corrects the mismatch (Figure 6).

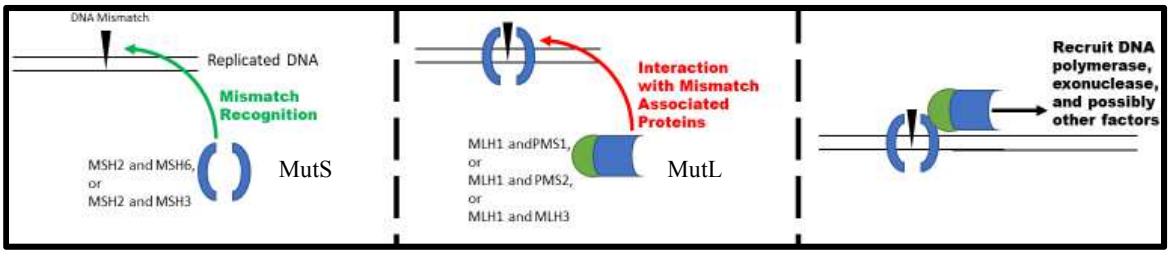


Figure 6. Recruitment and Function of Mismatch Repair Proteins

A DNA Mismatch is first recognized by a complex comprised of MSH2 and either MSH6 or MSH3, referred to as MutS. This complex recruits a second complex comprised of MLH1 and either PMS1, PMS2, or MLH3, a complex referred to as MutL, to the mismatch site. There, it functions to recruit other downstream factors which excise the mismatched DNA, polymerize new DNA, and perform other maintenance functions.

While only *MSH2* and *MSH6* were genes that were indicated to be heavily relied upon in MSS *POLE* mutant cells, mutations in many MMR genes are seen to promote cancer development when combined with *POL* mutations (Haradhvala et al., 2018). Cells with mutations in *POLE* which decrease the fidelity of replication would undoubtedly rely heavily on this process, and mutations in the MMR pathway are sensible secondary mutations on the path to tumorigenesis. However, tumors in MSS contexts forego this secondary mutation and hence, must have secondary mutations elsewhere that assist in an increased mutational rate. They must therefore likely rely on the MMR pathway to reduce mutational burden, lest it become deleterious to the genome.

Fanconi Anemia Genes.

The FA genes have less canonical linkage to Pol mutations but do play a major role in DNA repair, and thus also play a role in the development of cancer. FA genes function in the resolution of interstrand cross link (ICL) damage, but also play a role in homology driven repair at double strand breaks and fork stability (Lopez-Martinez et al. 2016). At least 23 genes are involved in FA pathway, including the well-known *BRCA1* and *BRCA2* as *FANCS* and *FANCD1* (Kolinjivadi et al., 2020). These 23 genes fall within 3 groups, categorized by their function: The first being the FA core complex, the second being FANCD2/FANCI, and the third consisting of nucleases, TLS polymerases, and homologous recombination factors. The core complex acts to recognize ICL and monoubiquitinate FANCD2/FANCI, which clamps to the DNA strand and recruits factors from the third group for resolution of the damage.

FANCM, the FA gene indicated to be heavily relied upon in MSS *POLE* mutants, interestingly falls somewhere in-between the first and third group. It acts to recruit the

core complex to DNA and therefore has a role in the monoubiquitination of FANCD2, but also acts as a translocase and functions in the bypassing of DNA lesions and the resolution of ICLs (Whitby, 2010). While the interaction between *POLE* mutations and FANCM is less clear than *POLE* mutations and the MMR pathway, the role of FANCM in error-free bypass of DNA lesions indicates an interesting possible link between the two genes.

ATR in Replication and DNA Damage Response

Ataxia-telangiectasia mutated (ATM) and ATM- and Rad3-Related (ATR) are central regulators in the DDR pathway, acting downstream of DNA damage sensors in both FA and MMR pathways and functioning to phosphorylate and regulate hundreds of proteins involved in DDR (Maréchal & Zou, 2013). While the ATM kinase functions mainly in response to double-stranded breaks (DSB) in DNA, ATR has more global functions in terms of responding not only to DNA damage, but also to replication stress caused by slow or stalled DNA replication (Zou, 2007).

ATR plays a key role in limiting replication stress at the replication fork by responding to slowed or stalled replication forks. Replication stress can be caused by a multitude of factors including unregulated replication speed, blockage of the replication fork by DNA lesions, ssDNA gaps, or secondary structures, and incorporation or encounters with ribonucleotides in the template DNA (Maya-Mendoza et al., 2018; Zeman & Cimprich, 2014). At a stalled replication fork, single-stranded DNA (ssDNA) near the replication machinery is bound by ssDNA binding protein-Replication Protein A (RPA), serving as a platform for the activation of ATR and thus triggering the phosphorylation and activation of hundreds of downstream substrates including Chk (Zou & Elledge, 2003). Phosphorylated Chk1 functions to slow DNA synthesis by reducing the firing of new

replication origins, thus allowing for the repair and recovery of stalled replication forks (Simoneau & Zou, 2021). ATR itself also functions to recruit and activate many downstream DDR factors for the resolution of various sources of genomic stress. In addition to replication stress, ssDNA generated by the action of nucleases at the sites of DSBs also recruits ATR, making this kinase a versatile protector of genomic integrity (Saldivar et al., 2017).

The Role of ATR in the MMR Pathway

With the MMR pathway indicated to be heavily relied upon in *POLE* mutant cells and ATR functioning as a critical kinase in the integrity of the genome, intersection between the MMR and ATR warrants investigation. After the recognition of a mismatch by MutS and the recruitment of MutL to the mismatch site, both MutS and MutL have been suggested to function as scaffolding for ATR recruitment and activation, as well as the recruitment of other ATR associated proteins such as TOPB1 (Y. Liu et al., 2010). In addition to these MMR factors acting as protein scaffolds, RPA is known to be recruited to mismatch sites and might play a role in the activation of ATR signaling at these sites (Guo et al., 2006). Ultimately, the role of ATR in MMR is not well characterized, and there are many questions that still remain regarding the function of ATR in the process of MMR and resolution (Z. Li et al., 2016). However, it has been shown that the MMR-mediated processing of certain mismatches generates replication stress, which is exacerbated in the absence of ATR-Chk1 activation (Gupta et al., 2018). This indicates a direct relationship between the MMR pathway and ATR signaling and suggests that cells dependent on the MMR pathway might be sensitive to ATR inhibition, thus offering ATR as a possible therapeutic target in *POLE* mutant cells.

The Role of ATR in the FA Pathway

FANCM is also indicated to be a genetic dependency in *POLE* mutated cell lines, and it has been shown that FANCM is essential for the efficient activation of ATR (Schwab et al., 2010). FANCM is involved in the resolution of both ICLs and stalled replication forks, and ATR-Chk1 activation play a role in both of these pathways (Basbous & Constantinou, 2019). In the case of ICLs, FA core complex formation at the site of DNA damage has been shown to be dependent on ATR, with FANCM being indicated as the key factor in ATR recruitment (Castella et al., 2015). Although the precise mechanism for ATR recruitment to the FA core complex is yet to be elucidated, FANCM has been determined to be phosphorylated directly by ATR in response to genotoxic stress (Singh et al., 2013). This interaction has been shown to play a role in the accumulation of FANCM at ICL sites as well as ATR-Chk1 signaling. FANCM is also implicated to interact with ATR at stalled replication forks independently of the FA core complex, with ATR being central to the recruitment of FANCM at ICLs (Ling et al., 2016). These combined studies show a reliance on ATR for FANCM function and indicate ATR as a possible therapeutic target in cells with a FANCM dependency.

Modeling *POLE* Mutations

In order to investigate these genetic dependencies and test treatments for them, we must generate a model system that would best suit these aims. As indicated by the hypermutator phenotype of mutated *POLE*, patient tumors with *POLE* mutations have high genetic variation. Hence, while there is a rich pool of genetic dependencies that stem from that, there may also be a diversity within these tumors, making the results difficult to interpret (Li et al., 2018; Temko et al., 2018). *POLE* mutants discovered in patient-derived

tumors can be used to identify the mutations seen in human physiology, but determining their pathogenicity and confirming mutator phenotypes needs the use of other model systems (Galati et al., 2020; Hamzaoui et al., 2020). Since the roles of Pols are evolutionarily conserved in eukaryotes, *Saccharomyces cerevisiae* makes an excellent model when determining if a mutation in *POLE* will cause a hypermutational phenotype (Miyabe et al., 2011). This is critical when determining the pathogenicity of a mutation seen in a tumor, since there are many different mutational variants of Pols seen in tumors and it is not always certain that these mutations will cause misincorporation of nucleotides during replication (León-Castillo et al., 2020).

While using *S. cerevisiae* is critical to determine the pathogenicity of *POLE* mutations, it functions poorly as a model when investigating treatments, and so we must identify suitable human cells in which to model the $POLE^{P286R}$ mutation. The human cancer cell line U2OS is MSS and has a low mutational burden of 8.167 mutations per Mb, and retains wild-type *TP53* status (van der Meer et al., 2019; Yang et al., 2013). U2OS cells are also polyploid, being listed as having 3.035 copies of each chromosome, which will be helpful in the modeling of a mutation that causes a hypermutational phenotype as polyploidy is theorized to operate as a "genetic buffer" in cells with high mutational burden (Kuznetsova et al., 2015; Li et al., 2020). The MSS context of U2OS will allow us to model $POLE^{P286R}$ without concurrent deficiencies in the MMR pathway, and owing to the relatively low mutational burden of the cancer cell line prior to *POLE* mutation, there should be a dramatic shift in mutation rate, as a rate of >10 mutations per Mb is to be expected with the generation of exonuclease-deficient Pol ε (Park & Pursell, 2019). These factors make U2OS a favorable human cell line in which to model the $POLE^{P286R}$ mutation.

Generating Knock-in Mutations Using Cas9

The human cell line U2OS with a heterozygous *POLE*$^{P286R/+}$ knock-in functions to model our mutation when investigating the genetic dependencies of MSS cells with *POLE* mutations. To generate this model system, we relied on CRISPR-Cas9 mediated gene editing. As a quick background on CRISPR-Cas9, this technology relies on recombinant Cas9 enzyme localized to the nucleus, a synthetic guide RNA (sgRNA) targeting the desire *POLE* locus, and a single-stranded oligodeoxynucleotides (ssODN) to serve as a template strand for repair. The Cas9 enzyme allows us to make a site-directed double-stranded break and is guided to the target gene where we intend to induce a knock-in using the sgRNA. After the DNA is cut, if homology-driven repair is used to repair the DSB, a single strand of DNA will be digested on each end of the break. Then the ssODN coding for the *POLE*^{P286R} knock-in mutation will be used as a template for the repair of the gene, yielding cells with our desired mutation (Doudna & Charpentier, 2014).

CRISPR-Cas9 Knockout Screening

In order to test if the genetic dependencies predicted by computational analysis of patient-derived MSS *POLE* mutant cells are indeed synthetic lethal targets in *POLE*$^{P286R/+}$ mutant U2OS cells, we intend to perform a DDR-focused CRISPR knockout screen in our generated models. This screening technique developed within the past decade targets multiple genes using multiple sgRNAs per gene to assure reliable knockout of the gene, and aims to knockout a single gene per cell (Doench et al., 2016; Shalem et al., 2014). This process makes use of plasmids encoding antibiotic resistance selection markers that express guides targeting the genes of interest, delivered to the cells by lentiviral vectors. This array of plasmids, called a library, encodes for guides targeting roughly 500 DNA damage

response genes, 20 non-DNA damage negative control genes, and includes 100 non-targeting guides, all chosen from previously validated library screens (Table 1, Appendix). Cells are treated with this library at a M.O.I. that ensures the likelihood that a single sgRNA is expressed per cell, and after a period of antibiotic selection that eliminates the cells not containing a plasmid expressing a guide, Cas9 expression is induced by the addition of doxycycline, thereby knocking out the gene target encoded by the sgRNA sequence. After a threshold of population doublings to allow cells with reduced viability to drop out of the pooled population, genomic DNA (gDNA) is collected and barcoded gRNA integrations then PCR-amplified, purified, and finally sent for next-generation sequencing. The resulting sequencing reads are then run through a ranking algorithm to determine which genes are essential to the $POLE^{P286R/+}$ cells when compared to the wild-type by assessing enrichment or depletion of guides in $POLE^{P286R/+}$ cells (Figure 7).

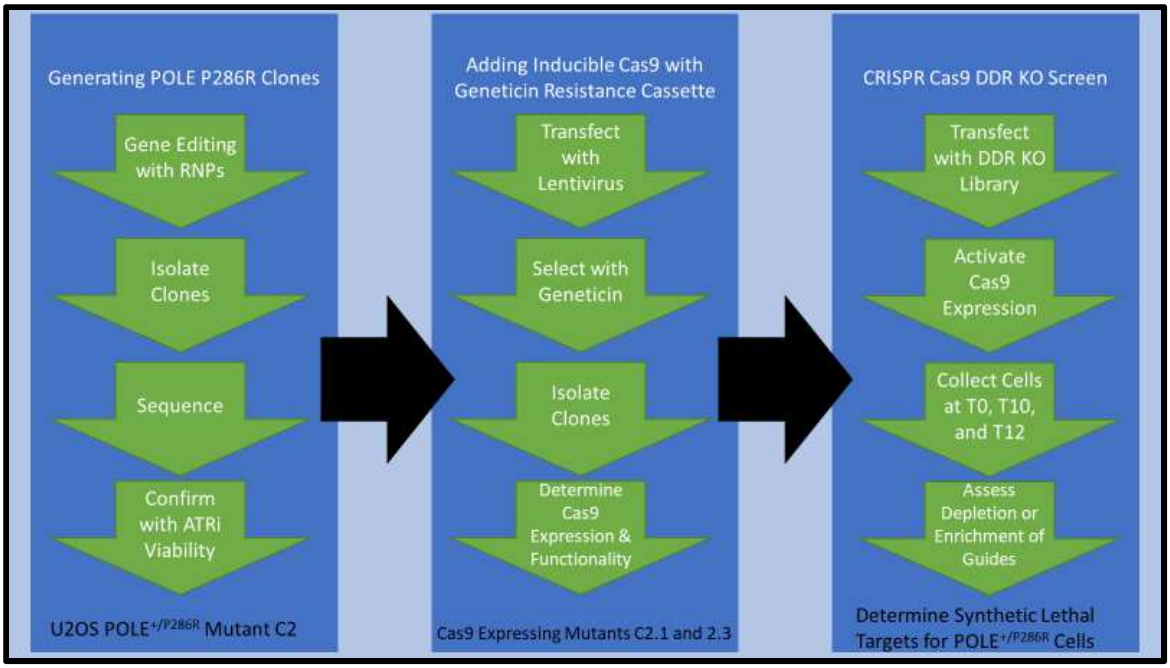


Figure 7. Workflow of Thesis

The workflow of this thesis project was to be separated into three phases: Generating and testing the $POLE^{P286R/+}$ *clones, transfecting and determining functionality and expression of inducible Cas9, and performing and assessing the CRISPR-Cas9 DDR KO Screen.*

Research Aims, Goals, and Hypothesis

Research from our lab indicates multiple genes, including *FANCM*, *MSH2*, and *MSH6*, are more heavily relied upon in MSS tumors with *POLE* mutations compared to those without *POLE* mutations. Hence, there are multiple avenues to investigate when determining which DDR pathway becomes more relied upon for cell survival in *POLE* mutant tumors. We aim to generate and validate cell lines with the $POLE^{P286R/+}$ mutation using CRISPR-Cas9, and Olaparib and VE-821 inhibitors to investigate our mutations. We also aim to knockout genes in the DDR pathway by means of a DDR-focused CRISPR knockout screen and identify druggable targets based off of our generated cell lines.

Therefore, we hypothesize that *FANCM*, along with other genetic dependencies to be identified by forward genetic screenings, will prove to be potent synthetic lethal targets, which will be assayed as a function of increased cell death in the generated $POLE^{P286R/+}$ cell lines when compared to isogenic wild-type cells.

Primary objective: Generate clonal population(s) of $POLE^{P286R/+}$ mutants and investigate the pathways that these cells depend on to compensate for their erroneous replication.

Specific Aim 1: Generate clonal populations and test their sensitivity to PARP and ATR inhibitors.

Methods: Generate $POLE^{P286R/+}$ mutants using CRISPR-Cas9 knock-in method, expand the clones, and validate the mutation by sequencing, then treat the generated cell lines with inhibitors and determine viability and perform DNA fiber analyzes.

Expected results: $POLE^{P286R/+}$ mutants will have shorter fiber tract lengths and a decreased viability when compared to WT controls.

Specific Aim 2: Determine synthetic lethality by performing DDR targeted CRISPR-Cas9 KO screen.

Methods: Target 500 genes intended for knock-out with RNA guides and determine enrichment or depletion of these sgRNAs using next-generation sequencing.

Expected results: *FANCM*, *MSH2*, *MSH6*, and possibly other genes involved in the DDR pathway will be depleted in $POLE^{P286R/+}$ mutants when compared to the WT controls, indicating a dependency on those genes.

Chapter II.

Materials and Methods

POLE$^{P286R/+}$ Mutant Generation

U2OS cells were selected to generate the model for our genome-wide screen. These cells require DMEM supplemented with 10% FBS and 100 I.U./mL of penicillin and 100 µL/mL streptomycin (Gibco), with this media being referred to as complete media. Once sufficient cells were cultured, conditioned media that the cells had been growing in was collected in a 15 mL centrifuge tube to assist in the recovery of the cells. The cells were then incubated with trypsin (Gibco) to dissociate them from the culture plate, transferred to a 15 mL centrifuge tube containing media to deactivate the trypsin, and centrifuged at 1,200 rpm for 3 minutes for pelleting. The cells were then resuspended in complete media and a sample was taken and placed in Nexcelom Bioscience Cellometer slides for cell counting using the Nexcelom Auto T4. For the genome editing of the U2OS cells, Lonza Cell Line Nucleofector Kit V was used, supplying the nucleofection solution, the supplement, and the electroporation cuvettes used in this procedure. HiFi Cas9-3xNLS was diluted to 20 pMol/µL in 2.4 µL and was incubated with 2 µL of gRNA diluted to 50 pMol/µL prior to electroporation. The RNPs were combined with 1 µL of ssODN diluted to 100 pMol/µL, then the solution was brought to a final volume of 20 µL using the supplied nucleofection solution (see Appendix for guide and ssODN sequences). 250,000 cells were removed from the previous 15 mL centrifuge tube and pelleted once again, then resuspended in the nucleofection solution and electroporated in the Lonza nucleofector 2b

using the "U2OS" program. The electroporated cells were cultured overnight in the collected conditioned media prior to isolation by dilution. To isolate the clones, cells were diluted to 0.3 cells per well containing complete media in a 96 well plate to ensure few wells had duplicate clones, followed by visual confirmation over the course of culturing. Once a clone became confluent in the 96 well plate, they were dissociated and transferred to a 6 well plate where they were cultured until they again became confluent. Once the clone reached confluence, the cells were dissociated in 500 µL of trypsin and collected in a 1.5 mL microcentrifuge tube containing 1 mL of complete media to deactivate the trypsin. 500 µL of the collected cells were then transferred to a second microcentrifuge tube, with the first microcentrifuge tube containing 1 mL of cells being stored for later culturing and the second microcentrifuge tube containing 500 µL of cells to be used for genotyping, described later. The cells to be frozen for culture were pelleted, resuspended in complete media supplemented with 10% Dimethyl Sulfoxide (DMSO), and transferred to a cryotube to be placed on ice for roughly 5 minutes prior to freezing at -80°C.

With our clones isolated, we then needed to determine which of the cell lines had our desired mutation. This required primers that target the site that we were interested in mutating, PCR master mix, samples from cells that we were interested in sequencing, agarose gel, an electrophoresis tank, and an imager that could identify the presence of DNA bands when labeled with ethidium bromide. We designed primers using the NCBI Primer-BLAST tool by uploading a FASTA sequence to the website and choosing between multiple primer pairs with a high likelihood of success. The primers were ordered from Integrated DNA Technologies (IDT) and tested for effectiveness using a U2OS cell line that had not undergone mutation or clonal separation and expansion.

To prepare the cells to be used as a template for PCR, they were dissociated by trypsin, transferred to a 1.5 mL microcentrifuge tube containing complete media to deactivate the trypsin, pelleted for 3 minutes at 10,000 rpm, and then washed twice with 1 mL of phosphate-buffered saline (PBS) with the same pelleting step in-between each wash step. After the final wash step, the U2OS cells were pelleted and frozen at -20° C until they were used for PCR, at which point the cells were resuspended in 100uL of UltraPure nuclease-free distilled water (Invitrogen) and were then heated to 95°C for 20 minutes, after which they were cooled by placing them on ice. We then combined 25 μL of NEBNext High-Fidelity 2X PCR Master Mix (New England Biolabs or NEB) with 10 μL of our U2OS template and 10 μL of nuclease-free distilled water, along with 2.5 μL of each forward and reverse primer, which at a 10 μM concentration using nuclease-free distilled water for dilution, yielding a final volume of 50 μL. We then placed the PCR tubes into a Bio-Rad C1000 Thermocycler and ran a program based on the recommended settings from New England BioLabs:

- Initial denaturation at 98°C for 30 seconds;
- Denaturation for 5 seconds;
- Anneal at 59°C for 30 seconds;
- Synthesize at 72°C for 20 seconds;
- Return to the 5 second denaturation step to repeat the cycle a total of 35 times;
- Elongation at 72°C for 2 minutes.

The amplified portion of DNA could then be tested using DNA electrophoresis to determine which primer pair had the highest amount of amplicon. Our lab generated our own 50x Tris Acetate-EDTA (TAE) buffer, which can be diluted to 1x for use during

electrophoresis. To formulate this buffer, we first formulated a 0.5 M ethylenediaminetetraacetic acid (EDTA) solution. For the EDTA solution, we dissolved 93.05 g of EDTA disodium salt into 400 mL of Milli-Q purified biology grade water, then adjusted the pH of the solution to 8.0 pH using sodium hydroxide, adding purified water to a final volume of 500 mL. Separately, we dissolved 242 g of Tris-base in 700 mL purified water, adding 57.1 mL of acetic acid and 100 mL of the formulated 0.5 M 8.0 pH EDTA, adding purified water to a final volume of 1 liter. This 50x TAE buffer was diluted to 1x and used to make agarose gel by adding 4 g of Lonza SeaKem LE agarose powder to 200 mL of 1x TAE buffer. The powder and buffer were heated in a microwave for 3 minutes, after which it was cooled to a handleable temperature and 10 μL of 0.0254 M ethidium bromide was added. This liquified gel was poured onto a mold with a removable well comb and allowed to solidify. Once solid, the gel was submerged in an electrophoresis bath containing 1x TAE buffer. The first well was loaded with a 1 kb plus ladder (NEB) labeled with a 6x purple gel loading dye (NEB) to determine the base pair length of the amplicon. We then added 2 μL of the gel loading dye to 10 μL of each PCR product, then loaded 10 μL of the labeled PCR product to the wells. The gel was run for 3 hours, after which a BioRad ChemiDoc imaging system was used to determine band intensity. We then selected the primer pair with highest intensity to continue with sequencing. To further enhance the PCR process, we optimized the annealing step for these primers by running the program on a gradient from 58°C to 70°C. We ran the PCR products on a gel using DNA electrophoresis and determined that 60.5°C was the optimal temperature for annealing based on band intensity.

Using the established primer pair, we then began to genotype our edited U2OS clones. Each of the clones that had been cryopreserved earlier had also had a portion of the cells washed and stored for genotyping. Those genotyping samples were prepared for PCR in the same method as the untreated U2OS cells, using 50 μL of nuclease-free distilled water instead of 100 μL due to the smaller number of cells collected. We performed PCR using the same method and thermocycler as previously described, using 60.5°C for the annealing temperature. We then isolated the amplicon by using Qiagen's PCR purification kit, adding 200 μL of buffer PB to 40 μL of PCR product in a QIAquick column and centrifuging at 13,000 rpm for 1 minute, washing by adding 750 μL of buffer PE and centrifuging at 13,000 rpm for 1 minute, discarding the flow-through, and centrifuging again for the same speed and time, then transferring the QIAquick column to a 1.5 mL microcentrifuge tube and eluting using 50 μL of EB buffer and centrifuging at 13,000 rpm for 1 minute. We then checked the concentrations of the amplicons using a Nanodrop 2000c spectrophotometer to determine if there was sufficient amplicon for sequencing, diluting or repeating the PCR process as necessary to account for deficiencies in amplicon concentration. We used the remaining 10 μL of PCR product to determine if the PCR was successful using DNA electrophoresis. The electrophoresis process was run for each of the clones to determine if the PCR was successful before sending the clones to be sequenced.

MGH uses its Center for Computational and Integrative Biology DNA Core for the sequencing process, and so that is where the amplicons were sent for sequencing. Initially, amplicons for each of the isolated clones were sent to be Sanger sequenced using the Core's Applied Biosystems BigDye v3.1 Cycle Sequencing Kit to determine if the amplicons

contained the desired mutation. The coarser results from Sanger sequencing indicated that clones 2, 6, 10, and 21 warrant further genotyping to be certain of their mutation, and so were again sent to the MGH DNA Core, this time for next generation sequencing for higher resolution using the Illumina MiSeq, along with their bioinformatics team for analysis. This round of sequencing identified clones 2 and 6 were heterozygous for the *POLE*^{P286R} mutation, hereafter referred to as C2 and C6.

Before moving forward in our work, we needed to confirm that our cells were free of contaminants. A common contaminant of cells that can misconstrue results is mycoplasma, and so to be certain that any further work that we do would not be affected by the bacteria, we tested our clones using ABM's Mycoplasma PCR Detection Kit (Nikfarjam & Farzaneh, 2012). Following the test kit's protocol, cells were cultured for 48 hours to reach 100% confluence, prior to collecting media for testing. In a slight modification of the protocol, 500 µL of media was collected from the culture into a 1.5 mL microcentrifuge tube and centrifuged for 1 minute at 2,000 g. 400 µL of supernatant was transferred in sterile conditions to a separate microcentrifuge tube and centrifuged for 10 minutes at 16,000 g. 350 µL of the supernatant was discarded and the pellet was resuspended for our template. For our PCR, we combined 12.5 µL PCR Master Mix, 1 µL primer mix, and 9 µL of nuclease-free water with 2.5 µL of positive or negative controls, all supplied by ABM, and 2.5 µL of our sample. After briefly mixing and centrifuging the PCR tubes, we again modified the supplied protocol by running the reactions by denaturing for 5 minutes, with additional denaturing for 30 seconds at 95°C, annealing at 55°C for 30 seconds, synthesizing at 72°C for 60 seconds, then returning to the second denaturing step for a total of 40 cycles, with a final synthesizing step for 10 minutes. The amplicons were

then electrophoresed on an agarose gel for 1.5 hours and indicated that there was no mycoplasma contamination in our culture.

Confirmation of Phenotype

With the genotypes of the two clones confirmed, we looked to determine cell sensitivity induced by the mutated Exo domain. To that aim, a 4-day ATR inhibition assay was used to detect viable cells after 4 days of culture with increasing concentrations of ATR inhibitor VE-821. First, an opaque-walled 96 well plate was seeded with C2, C6, and WT cells with 1,600 cells per well in 100 μL of media. 200 μL of sterile PBS was added to the peripheral wells to reduce evaporation in the wells containing cells. 24 hours later, VE-821 was diluted in 100 μL of media and was added to the wells in increasing dilutions from 1 to 40 μM so that the final volume of media in the well was 200 μL and the final concentrations of VE-821 in the wells ranged 0.5 to 20 μM. The cells were then cultured for 4 days, after which the viability of the cells was determined by Promega's CellTiter-Glo assay, which involves lysis of cells by addition of the provided reagents, followed by the measurement of ATP as an indicator of the number of viable cells present at the time of lysis. Briefly, the cells were equilibrated to room temperature for 30 minutes before adding 100 μL of the mixed reagents to each well. The plates were then shaken for 1 minute, left at room temperature for 10 minutes, and luminescence was determined using a PerkinElmer EnVision 2103 Multilabel Plate Reader and the EnVision Manager software.

Transduction and Functionality Screening of Inducible Cas9

After our cell line was confirmed to have the expected phenotype indicative of *POLE*$^{P286R/+}$, the next phase of the process was to generate stable and inducible Cas9 expression in the cells via lentiviral transduction. To do that, a method for transfecting the cells with the Cas9 gene as well as a method for selecting cells that contained the Cas9 gene would be necessary. Using a plasmid backbone of pInducer20 (pInd20), restriction enzymes were used to create "sticky ends" on both the Cas9 gene and the plasmid, after which there was a period of incubation to allow for annealing. This plasmid, created by Dr. Jian Ouyang in the lab, was what we used for packaging into lentiviral vectors. Next, we began production of lentiviral vectors that could deliver this pInd20-Cas9 plasmid to our *POLE*$^{P286R/+}$ cells. The combination of packaging vector PAX2 and the envelope vector VSV-G in HEK293T cells produced viral stocks containing our plasmid of interest, pInd20-Cas9. To perform this procedure, these cells had their media replaced by Opti-MEM (Gibco) and returned to the incubator while the vectors were being prepared. The lentivirus mastermix, packaging vector PAX2 with envelope vector VSV-G, both sourced from Addgene, were combined with our pInd20-Cas9 plasmid in a 15 mL centrifuge tube and diluted in 7 mL of Opti-MEM. In a separate centrifuge tube, 7 mL of Opti-MEM was mixed with 320 μL of lipofectamine (Invitrogen) and allowed to incubate at room temperature for 5 minutes. DNA was then added dropwise into the lipofectamine-Opti-MEM mixture and incubated for an additional 20 minutes at room temperature. After incubation, the vectors were added dropwise to the HEK293T cells before they were returned to the incubator. 48 hours later, the supernatant from these cells was collected

and tested for viral load before filtering the media through a 0.45 μm filter by syringe and storing at -20°C until transduction.

This lentiviral vector containing the pInd20-Cas9 plasmid was then used to transduce C2 and WT cells. After lentiviral transduction, the cells were allowed to recover for 24 hours before initiating selection for transduced cells via Geneticin G418 Sulfate antibiotic (Gibco). The concentration of G418 Sulfate was 1 mg/mL and the selection process lasted for two weeks, with cells being passaged as needed during the selection process. Afterwards, the subpopulations of clones were isolated by dilution similar to the previous process of clonal isolation, with 17 C2 and 10 WT subclones being isolated and cryopreserved after expansion. Once sufficient clones were isolated, the subpopulations were revived and tested for Cas9 expression during 24-hour culture with either 2 ug/mL doxycycline (Thermo Scientific) or no treatment. After culture with doxycycline, cells were collected for western blotting to determine the intensity of Cas9 expression in each subpopulation. Similar to collection for genotyping, the cells were trypsinized, collected into a microcentrifuge tube containing media to neutralize the trypsin, and washed twice with PBS. Cell pellets were then stored at -20°C until thawing in preparation for western blotting.

To prepare the cells for western blotting, they were first lysed with SDS protein extraction buffer, then the lysate must be tested for protein concentration for effective sample loading into the electrophoresis gel. This buffer was prepared by adding 2.5 mL of 1M Tris-HCl to 22.5 mL purified water for a 100 mM solution, then adding 0.5 g of SDS for a 2% volume to weight solution. 25 μL of this buffer was added to the cell pellets and pipetted to lyse the cells. The cell lysates were then sonicated for 10 minutes in a water

bath using a Qsonica Q800R3 to reduce the viscosity of the cell lysates. Using the Pierce BCA Protein Assay Kit, the BCA supplied in the kit was diluted in microcentrifuge tubes to 2, 1.5, 1, 0.75, 0.5, and 0.25 mg/mL to produce a protein standard. These standards, along with the lysate samples to be tested for protein concentration, were diluted 1:10 and 1:5 to a 10 µL final volume in microcentrifuge tubes to be certain that the range of protein present in the samples would fall within the range of the protein standard. Reagents A and B were mixed in a 1:50 ratio of reagent B in reagent A and 190 µL of the mixture was added to each sample and standard before they were incubated at 37^{o}C in a water bath for 30 minutes. After incubation, each tube was placed on ice to halt the reaction and the absorbency of the standards and samples were tested using the Nanodrop used to previously determine DNA concentration. The software supplied with the Nanodrop, also called Nanodrop 2000, first determined a standard curve based on the absorbency of the protein standards, after which the concentrations of the samples were mapped onto the standard curve based on absorbency. Lysate buffer was then added to the samples to reduce the protein concentration of all samples to 2 mg/mL, then a volume of 2x SDS buffer equal to the final volume of sample was added to each sample of lysate, reducing the final concentration to 1 mg/mL. The 2x SDS buffer also contained bromophenol blue in order to track the movement of the protein along the gel during electrophoresis.

The sample lysates were then loaded into Invitrogen 4-12% Bis-Tris Plus gels for electrophoresis. The gels were placed into mini gel tanks, the tanks were filled with Invitrogen MES SDS Running Buffer diluted to 1x, and 10 µL of samples were added to each of the wells with 7 µL of PageRuler Plus Prestained Protein Ladder (ThermoFisher) being added to one well to determine protein size. The samples were then run for 2 hours

at 85 volts at room temperature before being transferred to Immobilon-P PVDF membrane (Millipore) in transfer buffer for 2 hours at 90 volts at room temperature. The transfer buffer was produced in-lab by first making 10x transfer buffer by diluting 116 g of Tris and 586 g of glycine into 4L of purified water, then diluting that to 1x by adding 700 mL of purified water to 200 mL of methanol, then adding 100 mL of the 10x transfer buffer. After the proteins were transferred to the membrane, the membrane was blocked in 5% milk in Tris-buffered Saline (TBS) with 0.1% Tween-20 (TBS-T) for 20 minutes on a shaker at room temperature. The milk was removed and replaced with 5% milk in TBS-T containing primary antibodies targeted to Cas9 and GAPDH diluted 1:2,000 and 1:8,000 respectively and incubated at 4°C for at least 16 hours. After primary incubation, the primary antibodies were removed and the membrane was washed in TBST three times for 5 minutes on a shaker at room temperature, after which secondary antibodies diluted in 5% milk 1:5,000 were added to the membrane. The secondary antibodies targeted mouse antibodies and had horseradish peroxidase reporters, and the membrane was incubated with the secondary antibodies for 4 hours shaken at room temperature before the antibodies were removed and the membrane was again washed three times for 5 minutes. Bio-Rad Clarity Western ECL Substrate was applied to the membranes for 3 minutes before imaging in a Bio-Rad Chemidoc MP using the Bio-Rad Image Lab software to auto-expose the bands for imaging (Figure 8).

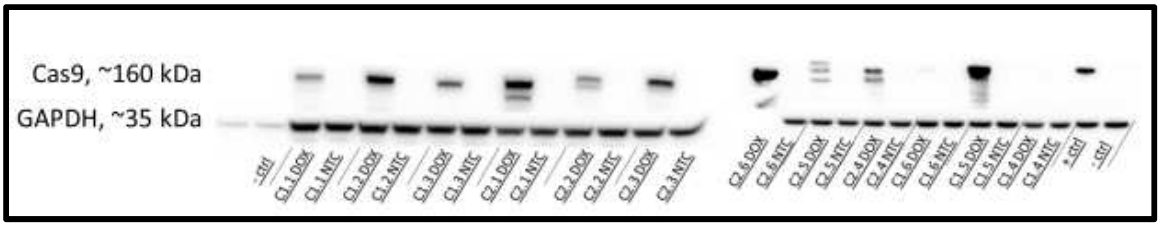


Figure 8. Inducible Cas9 Expression in Isogenic Controls and *POLE*$^{P286R/+}$ Cells

Inducible Cas9 expression in our isogenic controls and our POLE$^{P286R/+}$ *mutants was determined by western blotting after incubation with or without doxycycline for 24 hours. No clones had constitutive or "leaky" expression of Cas9, but clones 1.4 and 1.6 survived G418 sulfate selection without incubation with doxycycline inducing Cas9 expression.*

This Cas9 expression assay showed that WT subclones 1.2, 1.3, and 1.5 as well as C2 subclones 2.1, 2.3, and 2.6 had high levels of Cas9 that were only expressed in the presence of doxycycline in the culture media. However, while the expression of the Cas9 in these subclones were comparable, the functionality of the Cas9 protein needed to be tested in order to move forward with the transduction of the knockout library.

To determine if the Cas9 being expressed in our subclones was functional, *RPS19*, a gene necessary for maturation of the smaller of the two ribosomal subunits and thus the function of ribosomes, was selected as a site to be targeted to determine functionality of the Cas9 protein (Flygare et al., 2006). Lentiviral vectors were prepared containing constructs for sgRNA targeting *RPS19* following the protocol used for pInd20-Cas9 construct delivery. These viruses were applied to a population of each of the subclones that were previously determined to have high levels of Cas9 expression. Once the cells were transduced with these constructs, they began to produce the sgRNA targeting *RPS19*, but wouldn't be producing the Cas9 necessary for digestion of the *RPS19* gene unless they

were cultured with doxycycline. The subclones expressing sgRNA for *RPS19* were then cultured in two wells: one with 2ug/mL of doxycycline in the culture medium and one without. After 48 hours of culture, the cells were washed twice with PBS to remove any media or dead cells before being fixed with methanol for 10 minutes. The methanol was aspirated off and the cells were then stained with crystal violet solution in a 25% methanol solution for 10 minutes, after which the plates were washed of dye and imaged (Figure 9). Subclone WT 1.5 had a relatively low viability in the non-treatment well, indicating that there was possibly leaky expression of Cas9 that was targeting *RPS19* even without the induction of Cas9 with doxycycline. WT 1.2 had relatively high viability when cultured with doxycycline, indicating that the Cas9 being expressed might not be very functional in digesting DNA. WT 1.3 had high viability in the non-treatment well and low viability in the well treated with doxycycline, indicating that there was no expression of Cas9 without doxycycline, and that when the Cas9 was expressed, it effectively targeted and digested the *RPS19* gene, leading to cell death. All three selected C2 subclones had high viability in the non-treatment wells, indicating there was no expression of Cas9 without the presence of doxycycline in the media. Also, all three had reduced viability when cultured with doxycycline. However, subclones 2.1 and 2.3 had lower viability than 2.6 when cultured with doxycycline, indicating that those subclones had Cas9 that could more effectively target and cleave *RPS19*. Using this assay to determine effectiveness and inducibility of Cas9, subclones 1.3, 2.1, and 2.3 were selected as the WT control and two $POLE^{P286R/+}$ mutants to move forward with the knockout library screening.

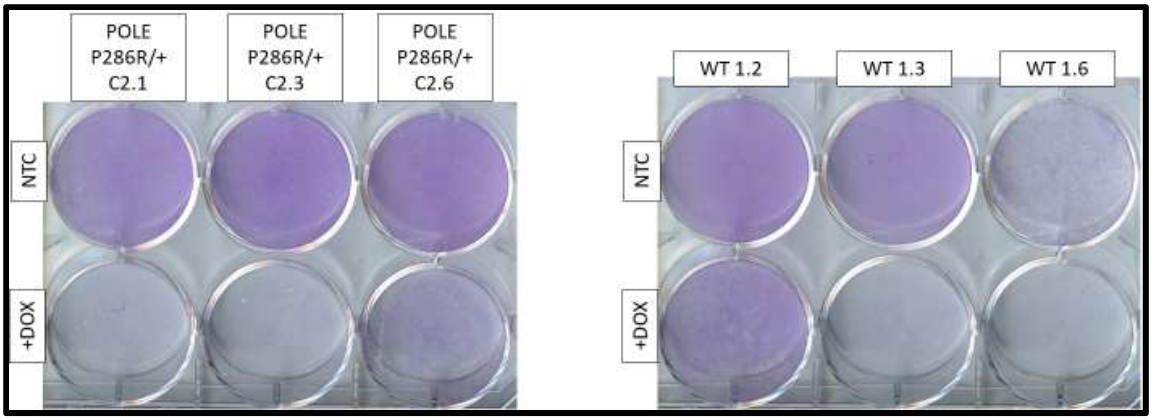


Figure 9. Cas9 Effectiveness in Targeting Critical Gene *RPS19*

Cells were cultured with either no treatment or doxycycline for 48 hours after being transduced with a plasmid expressing a guide for RPS19*, a gene critical for cell survival. The low viability in the NTC well of WT 1.6 cells indicates leaky expression of Cas9, while the high viability in doxycycline treated C2.6 and C1.2 indicates low functionality of the expressed Cas9 in those cell lines.*

DNA Fiber Assay

DNA fiber assays were performed to determine the effect of ATR and PARP inhibitors on replication fork progression of our mutants. The cells were seeded at 200,000 cells per well in a 6 well plate and allowed to grow overnight. The next day, the cells were treated with media containing a 50 μM concentration of CldU for 15 minutes, washed twice with media, then treated with media with a 100 μM concentration of IdU along with four different conditions:

1. 10 μM PARP inhibitor (PARPi) Olaparib, diluted in DMSO, and a volume of DMSO added equal to the volume of XL-413 added to other conditions

2. 10 μM ATR inhibitor (ATRi) VE-821 and 5 μM CDC7 inhibitor (CDC7i) XL-413, diluted in DMSO, and a volume of DMSO equal to the volume of Olaparib added to other conditions
3. 10 μM Olaparib, 10 μM VE-821, and 5 μM XL-413
4. A volume of DMSO equal to the volume of Olaparib and XL-413 added to other conditions

The cells were treated with the four different conditions for 60 minutes, after which the cells were trypsinized, collected in 1.5 mL tubes, washed twice with PBS, and resuspended in 100 μL of PBS. 3 μL of cell suspension was placed on individually labeled glass slides along with 7 μL of lysis buffer comprised of 200 mM Tris-Cl, 50 mM EDTA, and 5% weight per volume SDS at pH 7.4. The lysis buffer and cell suspension was mixed gently by pipetting and was allowed 3 minutes for lysis to occur before tipping the glass slides to spread the DNA fibers across the slide, then allowing the droplet to dry for roughly 30 minutes. The slides were then fixed with a 3:1 ratio of methanol: acetic acid in a -20°C freezer for 30 minutes, then dried overnight. The next morning, the slides were submerged in 2.5 M Hydrochloric Acid for 1 hour to denature the DNA, then washed three times in PBS for 5 minutes. The slides were then blocked in PBS with 0.05% Tween20 (PBST) and 2% bovine serum albumin (BSA) at 37°C for 1 hour to avoid non-specific binding of the antibodies. After blocking, the slides had excess blocking solution removed and were incubated with primary antibodies: Mouse anti-IdU diluted 1:50 in TBST with 1% BSA and sourced from BD Biosciences, and rat anti-CldU diluted 1:100 in the same tube and sourced from Novus. 50 μL of the primary antibodies were added to each slide, then the slides were incubated at 37°C for 1 hour. After primary incubation, the slides were washed

three times for 5 minutes in PBST before being treated with secondary antibodies (Jackson ImmunoResearch): anti-rat Cy3 reporter diluted 1:100 in PBST with 1% BSA, and anti-mouse Alexa Fluor 488 reporter also diluted 1:100 in the same tube. 50 μL of the secondary antibodies were added to each slide, then the slides were again incubated at 37°C for 1 hour. The slides were washed twice with PBST with a final wash of PBS for 5 minutes before they were allowed to dry covered for at least 30 minutes. After drying, 40 μL of ProLong Gold (Invitrogen) was applied to the slides, a cover slip was applied, and the resin was allowed to cure overnight before imaging using an Echo Revolve fluorescence microscope. The fluorescence images were superimposed and colored using a MatLab program written and executed by Dr. Antoine Simoneau, then a minimum of 150 fibers' lengths were measured using ImageJ and used to calculate fiber ratios for each of the conditions, with GraphPad Prism used for statistical calculations for comparing the fiber ratios.

DNA Damage Response Focused CRISPR-Cas9 Knockout Screen

Genes in the DDR pathway, DNA replication pathway, and mRNA production and modification pathways were chosen based on their roles in those pathways, and guides expressed by plasmids were used to target Cas9 to those genes. The guides were selected from pre-existing libraries including Avana, Sanger, Yusa, and Broad libraries, with 6 guides being selected per gene, and plasmids were used to express those guides. The plasmids used were sourced from Addgene, amplified in *E. coli*, and lentiviruses containing the plasmids were produced in accordance with the protocol developed by Joung et al. (Joung et al., 2017). The lentiviruses produced were applied to C1.3, C2.1, and C2.3 by counting out 10^7 cells per infection and adding viral supernatant at a MOI of 0.3, while 10^7 C1.3 cells were separated out to use as non-treated controls. After 24 hours of incubation,

the cells were washed and allowed to recover for 24 hours in DMEM before being treated with 2ug/mL of puromycin to select for transduced cells. The NTC cells were killed over the course of 4 days, indicating that cells that had not been transduced had been removed from the population. We then collected T0 cells for sequencing: 5.28 E+6 C1.3 cells and 3.2 E+6 C2.3 cells, while discontinuing the screen of C2.1 due to slow growth. The cells were then treated with G418 and doxycycline to continue selection and induce Cas9 expression and passaged to the point of 10 and 12 population doublings as determined by cell counting during passaging, with the minimum number of cells passaged maintained at or above 6.2 E+6 cells. During the time of passaging, a western blot using a similar protocol as previously described was performed on a sample of cells to confirm Cas9 expression (Figure 10). At the two timepoints of 10 and 12 population doublings, roughly 10^7 cells were collected for sequencing.

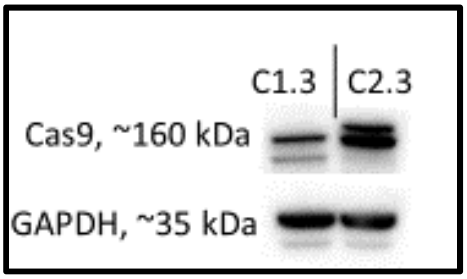


Figure 10.Cas9 Expression During KO Screen

To be certain that Cas9 was being expressed in our cell lines, Cas9 expression was again validated by western blotting.

The T0 cells were resuspended in 1.6 mL of TE buffer sourced from Invitrogen, then lysed by adding 50 µL of 20% SDS in UltraPure water and 5 µL of proteinase k

(Thermo Scientific) was added to halt any DNA degradation. T12 cells required double the volume of all components. The lysate was poured into a 15 mL centrifuge tube containing Qiagen MaXtract High Density gel and an equal volume of phenol-chloroform (Thermo Scientific), then spun at 2,500 g until the supernatant was clear and the phenol-chloroform containing other cellular contaminants was separated from the aqueous layer, which contained the gDNA. In a new 15 mL centrifuge tube, 2.5x the volume of supernatant in ethanol (Thermo Scientific) was added to 1/10 the volume of the supernatant of sodium acetate (Thermo Scientific). The gDNA containing supernatant was poured into the ethanol and the gDNA was precipitated, then collected and transferred to a 1.5 mL microcentrifuge tube. The gDNA was washed 3 times by pipetting 1 mL of 80% ethanol over the DNA and removing the excess by pipetting, then allowed to dry. After drying, the gDNA was diluted in 200 mL of TE buffer (Invitrogen) and 2 mg of RNase A (NEB) was added to each tube and to remove any residual RNA and further purify the gDNA. The DNA was then further dissolved by overnight incubation at 55°C. We then checked the concentration of the gDNA in the nanodrop and adjusted the concentration so that each 50 µL PCR reaction contained 2.5 µg of gDNA and ran a two-step PCR. The PCR functions to isolate and barcode the gRNA sequence with Illumina i5 and i7 barcodes, as well as to add additional barcodes within the sequence to deconvolute the multiplexed sample during sequencing. We then sequenced the amplified guides and used the screening analysis method 'Model-based Analysis of Genome-wide CRISPR/Cas9 Knockout' (MAGeCK) to determine the enrichment or depletion of guides relative to the isogenic controls (W. Li et al., 2014).

Chapter III.

Results

Viability Assay

To determine sensitivity to ATR inhibition, cell lines with *POLE*$^{P296R/+}$ mutations as well as a wild-type control were treated with 0, 2, 3, 5, 7.5, and 10 μM concentrations of VE-821. In determining the sensitivity to ATR inhibition in our clones, it was discovered that both mutant clones were more sensitive to VE-821 treatment when compared to the WT control. However, Clone 2 (C2), the clone with one out of three *POLE* alleles mutated, showed higher sensitivity to ATR inhibition when compared to Clone 6 (C6), the clone with two out of three *POLE* alleles mutated.

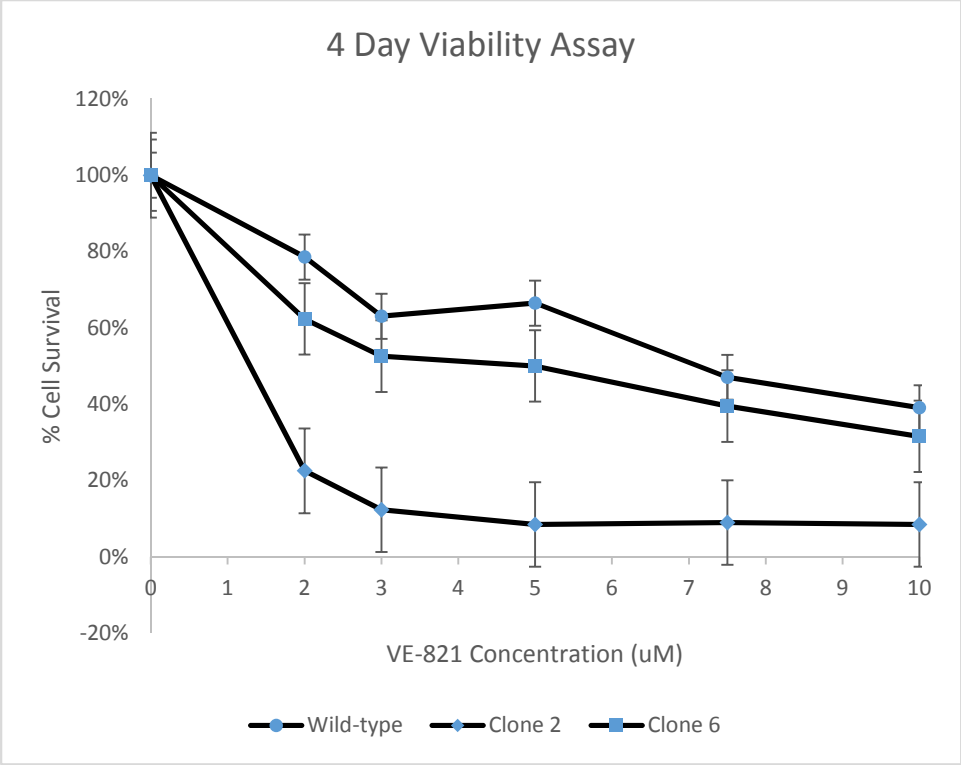


Figure 11.Viability Assay

$POLE^{P286R/+}$ cell lines and isogenic controls were treated with ATRi (VE-821) for four days and were compared to cells with no ATRi treatment. Data is represented as a group average with n=6, error bars showing one standard deviation.

DNA Fiber Assay

The rates of replication fork stalling during genomic stress were determined by labeling DNA fibers while incubating C2 and C6 along with a wild-type control with various inhibitory drugs. Olaparib was used to inhibit PARP and VE-821 was used to inhibit ATR. VE-821 and CDC7 inhibitor XL-413 were used in combination to limit the increase of new origin firing that accompanies the inhibition of ATR, since ATR functions to limit new origin firing during periods of replication stress.

The cells were incubated first with CldU for 15 minutes, then IdU and inhibitors for 60 minutes. The inhibitor treatments were 10 μM of PARP inhibitor (PARPi), 10 μM of ATRi and 5 μM of CDC7i, and all three inhibitors simultaneously. A minimum of 150 DNA fibers were measured and the ratio of the IdU fiber length divided by the CldU fiber length were taken for each fiber, then the ratios were compared for each condition using Mann-Whitney statistical analysis of the median values.

This analysis shows that there is a significant increase, a p-value of <0.05, in the average fiber length in C6, as compared to WT cells when the cell lines are incubated with PARPi. C2 also has an increase in the average fiber length, but the results are not statistically significant in this assay. Secondly, it shows that there is no significant change in the average fiber length when the cell lines are incubated with ATRi and CDC7i. Lastly, this assay shows that there is a significant difference in average fiber lengths for both C2 (p-value <0.001) and C6 (p-value <0.05) when the cells are incubated with PARPi as well as ATRi and CDC7i.

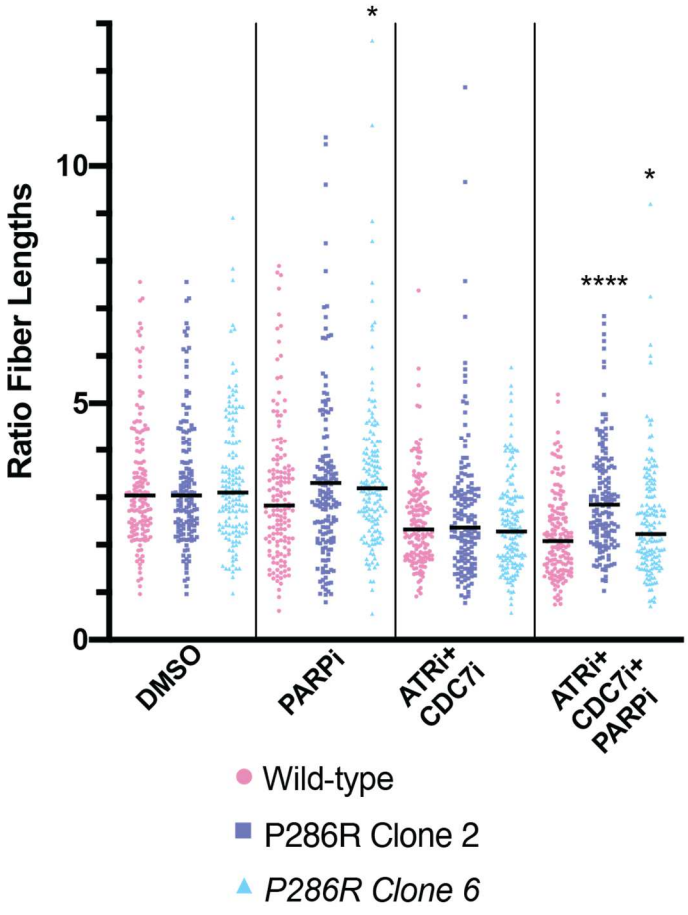


Figure 12.DNA Fiber Assay

Isogenic controls and POLE$^{P286R/+}$ *cell lines were incubated with CldU for 15 minutes, followed by IdU and inhibitors for 60 minutes. The inhibitor conditions were: PARPi Olaparib, ATRi VE-821 and CDC7i XL-413, and a combination of ATRi, CDC7i, and PARPi. At least 150 fibers were measured for each cell line in each condition. Lines represent the median value of the cell line's IdU:CldU ratio. *: $p<0.05$ and ****: $p<0.0001$ as assessed by a two-tailed Mann-Whitney statistical analysis of median values.*

Chapter IV.

Discussion

Significance of Results

Mutations in the proofreading domain of *POLE* are a common occurrence in endometrial, colorectal, and multiple other tumor types. This mutation is noted to be a driver mutation, causing a high mutational burden while also maintaining MSS status. In order to search for genetic dependencies in these cell lines, we have generated inducible Cas9 expressing $POLE^{P286R/+}$ mutants and probed them for cell sensitivity using inhibition of repair pathways and a DDR focused knockout screen. We used viability assays to determine the sensitivity of our clones to ATR inhibition, as well as tested replication fork progression and fork stalling during ATR and PARP inhibition by labeling the nascent DNA during treatment. The results of our pilot screen are pending NGS and analysis, and future work will serve to address putative target validation and mechanistic studies once genetic dependencies have been indicated

The generation of inducible Cas9 expressing $POLE^{P286R/+}$ clones was pivotal to the process of performing a DDR focused knockout screen. The generation of these clones was validated by the sequencing of *POLE* gene after knocking in the mutation, and also confirmed by increased cell sensitivity to ATR inhibition, and reduced fork stalling when treated with ATRi and PARPi. The inducible expression of functional Cas9 was also a critical portion of the model generation, and the expression and functionality of Cas9 was confirmed by western blotting and critical gene targeting, respectively. With these aspects

of our model confirmed, we have generated an adequate model to perform out knockout screen.

Our *POLE*$^{P286R/+}$ models were tested for their sensitivity to ATR inhibitor VE-821 by a four-day viability assay (Figure 11). When compared to isogenic controls, the mutant clones showed higher sensitivity after being treated with increasing concentrations of the inhibitor, although Clone 2 had a higher sensitivity to ATRi when compared to Clone 6. Sequencing of these clones showed that Clone 2 had 1 out of 3 copies of *POLE* with the P286R mutation while Clone 6 had 2 copies mutated, and unpublished data from other labs indicate that there is an unexplained downregulation of *POLE*^{P286R} expression in certain contexts. This is possibly due to detrimental effects of proofreading-deficient Pol ε, imposing selective pressure to preferentially express the WT gene, which may account for the reduced sensitivity in Clone 6. Therefore, it is plausible that there is more selective pressure in Clone 6 to downregulate mutant *POLE* expression due to increased mutant copy number relative to Clone 2. Due to this ambiguity, we opted to proceed with Clone 2 for the purpose of our DDR-focused screen. The sensitivity of Clone 2 may be attributed to the high misincorporation of nucleotides by the mutated Pol that must be corrected by MMR. MMR complexes MutS and MutL interact with components of the ATR-dependent damage response, with MutSα directly associating with ATR, CHK1, and TOPB1 and MutL associating with TOPB1 (Y. Liu et al., 2010). Indeed, it has been shown that the activation of ATR during MMR-mediated processing of misincorporations leads to increased cell viability (Gupta et al., 2018). While proofreading domain-deficient Pols may not cause DNA damage, the high misincorporation of nucleotides would likely cause an increase in the MMR activation, as observed by Gupta et al. Upon ATR inhibition, the

MMR process would be less functional and DNA damage may accumulate, leading to the observed DSBs and apoptosis. This suggests that our *POLE*$^{P286R/+}$ models are more reliant on ATR for cell survival, likely due to the role of ATR during MMR process (Figure 5).

Our *POLE*$^{P286R/+}$ models were also tested for replication fork stalling in the presence of PARP and ATR inhibition (Figure 12). This experiment found that *POLE*$^{P286R/+}$ cells were less sensitive to fork stalling caused by PARP and ATR inhibition when compared to isogenic controls, as well as a similar fiber length of DMSO treated cells (Figure 14, Appendix). When incubated with PARPi, the ratios between the first and second labeling slightly increased, which can indicate an increase in fork speed as well as a decrease in fork stalling in the mutant cell lines during the time of treatment. While both mutants showed an increase in DNA fiber ratios, this result is noteworthy due to Clone 6 having an increase of greater significance when compared to Clone 2, even when it was shown in the viability assay that Clone 2 had a higher sensitivity to ATRi and therefore a more pronounced phenotype. It is possible that the inhibition of mutant Pol ε in Clone 6 occurs in part by PARP-dependent mechanisms, as PARP is known to have a critical role in directly regulating Pol ε at replication forks (Merchut-Maya et al., 2019). Inhibition of PARP also increases fork speed, and it is possible that cells with mutated *POLE* exonuclease domains may have their fork speeds more readily increased by PARP inhibition (Maya-Mendoza et al., 2018). With the mutated Pol ε experiencing less inhibition by PARP, fork speeds could increase in Clone 6 as well as Clone 2, albeit at different levels. ATR inhibition, combined with CDC7 inhibition to reduce origin firing, appeared to reduce the ratios in all cell lines equally. This result is consistent with previous findings that ATR inhibition prevents the resolution and restart of stalled replication forks,

resulting in reduced fork rates (Simoneau & Zou, 2021). The addition of PARPi in conjunction with ATRi and CDC7i partially rescues the DNA fiber ratio in both Clone 2 and Clone 6, with Clone 2 having a much higher significance than Clone 6 when comparing the two to the isogenic control cell line. These results may be explained by the role of PARP in regulating the rate of fork progression, as well as *POLE*$^{P286R/+}$ cells having a higher propensity to increase fork speed in the presence of PARPi. This would indicate that direct interaction of PARP with Pol ε plays a major role in the regulation of fork speed. Indeed, it has been shown previously that PARP acts as a negative regulator of Pol ε in a dose dependent manner (Eki, 1994). The inhibition of ATR may slow fork speeds across all cell lines, irrespective of Pol ε status, but the inhibition of PARP in cell lines with proofreading domain mutations increases the replication fork speed. This would indicate that PARPi decreases the likelihood of fork stalling or reversal in *POLE*$^{P286R/+}$ cells. This could be an avenue of treatment worth pursuing, as it has been indicated in other tumor types that PARPi and ATRi treatments resulting in an increase in fork speed in the presence of genomic instability lead to an increased sensitivity to the genomic instability (Parsels et al., 2021). This result requires further confirmation however, as this fiber assay result was found difficult to replicate (Figure 15, Appendix).

Genetic Dependencies Generated from Cancer Dependency Databases

Due to our DDR KO screen pending sequencing for putative hits, we opted to make use of other methods for determining genetic dependencies in *POLE*-mutated MSS tumors. To achieve this, we have taken the top hits for genetic dependencies from the analysis performed by the Lawrence Lab, as well as genetic dependencies based on online databases DepMap and the Genomics of Drug Sensitivity in Cancer (GDSC). To continue with the

identification of synthetic lethal targets in *POLE*$^{P286R/+}$ tumors, we have selected cell lines generated from CRC and EC tumors that are MSS and have *POLE* mutations and determined the genes that are most heavily relied upon by either CRISPR KO, RNAi, or drug sensitivity (Table 2). This selection results in 5 cell lines: SNU-C1, SNU-81, SNU-1040, HT-115, and HCC-2998, all of which except SNU-1040 have had their essential genes determined by either CRISPR KO or RNAi and those results being available on the DepMap database. For SNU-1040, data showing genes essential to the cell line via CRISPR KO or RNAi are unavailable on the DepMap database, but the genes targeted by the five drugs that SNU-1040 are most sensitive to are available on the GDSC database (Yang et al., 2013). Using these two resources, we have determined overlapping essential genes among selected cell lines similar to our *POLE*$^{P286R/+}$ cell line and are using them as fill-ins for hypothetical genetic dependencies in our knockout screen.

Cell Line	Essential Genes Determined by CRISPR KO	Essential Genes Determined by RNAi	Essential Genes Determined by Drug Sensitivity
SNU-C1	KLF5	**CTNNB1**	
	STX4	DLG1	
	TUBB4B	*PLK1*	
	CTNNB1	SMC1A	
	NMNAT1	LEO1	
	MAP2K1	PFAS	
	FDFT1	ZNF101	
	FBXO11	**MYB**	
	PFAS	GPN3	
	MVD	RING1	
SNU-81	**CTNNB1**	**CTNNB1**	
	KCTD10	MED7	
	NMT1	PSMD2	
	SNAP23	*BIRC5*	
	APC	RPAP1	
	VPS13D	TRA2B	

	UBE2N	NCBP2	
	RNF4	SNRNP200	
	TDP2	DDX10	
	NSMCE3	CASP8AP2	
SNU-1040	N/A		JAK3
			AKT1, AKT2, AKT3
			PKCB
			EGFR
			ERK1, ERK2
HT-115	MYLIP	SCD	
	HNF1A	**CTNNB1**	
	MPHOSPH6	**BCL2L1**	
	TSC2	DHX9	
	PTDSS1	EFCAB8	
	UPF3B	NUP98	
	CNTROB	KNL1	
	CDK4	COPS8	
	CTNNB1	**MYBL2**	
	SRSF6	DLST	
HCC-2998	**TSC2**	N/A	
	NXT1		
	STX4		
	NMT1		
	BCL2L1		
	RIC1		
	TSC1		
	CFL1		
	GMPS		
	KRAS		

Table 1. Representative Cell Lines and Their Genetic Dependencies

Using DepMap and GDSC online databases, 5 cell lines were selected to represent the $POLE^{P286R/+}$ *cell line generated in this project. Adjacent to each of the selected cell lines are the essential genes determined by either CRISPR KO, RNAi, or drug sensitivities.* ***Bold*** *genes represent genetic dependencies that are overlapping with other selected cell lines,* italicized *genes are those that are downstream of the MYB gene family expression, and* <u>underlining</u> *represents genes involved in the autophagy pathway.*

As an initial step towards determining sensitivities of our selected cell lines, we used the GDSC website to determine the sensitivity of the selected cell lines to ATR inhibition, as we have determined that our *POLE*$^{P286R/+}$ models are sensitive by viability assay. When charting the data for the sensitivity of the selected cell lines, it didn't appear that any were deemed sensitive to direct ATR inhibition by either VE-821, VE-822, or AZD-6738 (Figure 13). The GDSC database determined a z-score of -2 or lower to be considered sensitive to a drug, and there were no cell lines that met that requirement. HCC-2998 was the cell line that had the highest sensitivity to ATR inhibition, with all three drugs reaching a z-score between -0.7 and -0.9, but multiple cell lines also showed mild resistance to the inhibitors, with SNU-81, HT-115, and SNU-1040 attaining a z-score range of 0.5 to 1.2 indicating resistance to ATRi treatment. This may indicate that direct ATRi treatment may not be the best option for our model and seeking alternative genetic dependencies may be an attractive option, further highlighting the utility of our DDR-focused screen. This could also indicate a difference in sensitivities between early-stage and late-stage *POLE* mutant cells, as our generated *POLE*$^{P286R/+}$ cells showed a marked increase in ATRi sensitivity when compared to isogenic controls (Figure 11). It is possible that as these cells transform, further mutations occur, such as in the MMR and FA pathways, which could cause a decreased reliance on DDR pathways. We must therefore look to treat these cell lines with different synthetic lethality targets to theorize which genes would be relied upon later in the *POLE*-mutated cell.

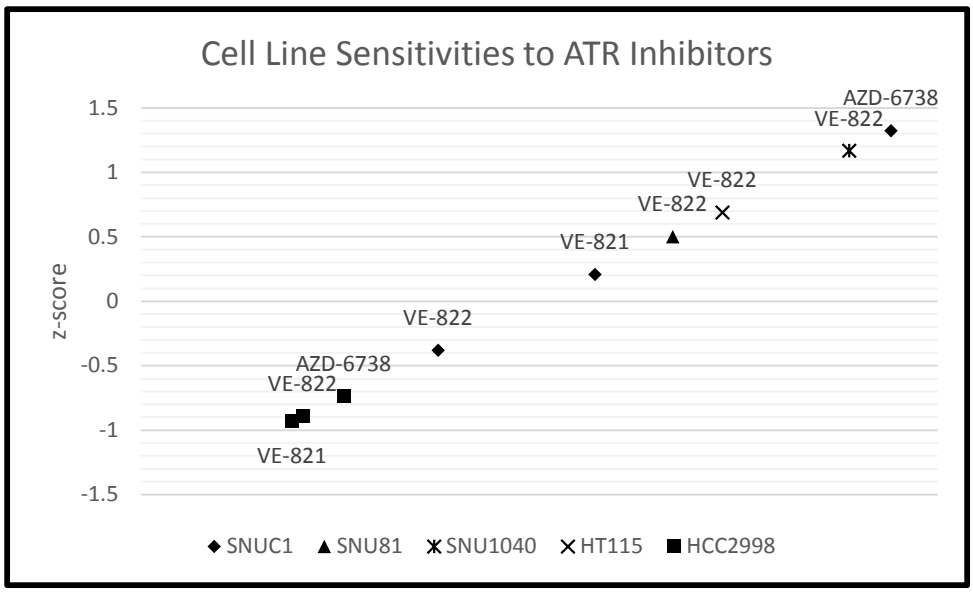


Figure 13. Cell Line Sensitivities to ATR Inhibitors

To investigate targetable pathways in our selected cell lines, we reviewed data regarding ATR inhibitor sensitivity available on the GDSC database. Cells were treated with inhibitors for 72 hours before determining a z-score of sensitivity based on the LD50 of the drug. As the GDSC website determines a score below -2 as sensitive and above 2 as resistant, none of the cell lines reach those standards.

In addition to using the Lawrence lab's analysis to determine *FANCM* and the MMR genes *MSH2* and *MSH6* as possible genetic dependencies present early in tumorigenesis in *POLE*-mutated MSS cells, we will be using overlapping essential genes identified in selected cell lines representing *POLE*-mutated MSS cells late in tumor development. As shown in Table 2, we used a rudimentary selection process to identify essential genes in multiple selected cell lines. The genes that are essential to two or more of the five selected cell lines are syntaxin 4 (*STX4*), β-catenin (*CTNNB1*), MYB family genes *MYB* and MYB-Like protooncogene 2 (*MYBL2*), N-myristoyltransferase (*NMT1*), BCL2-Like 1 (*BCL2L1*), and Tuberous Sclerosis Consortium 2 (*TSC2*). In addition, Polo-

Like Kinase 1 (*PLK1*) and Baculoviral IAP Repeat-Containing Protein 5 (*BIRC5*) genes are relevant downstream targets of MYB family genes, and Janus Kinase 3 (*JAK3*), Akt Serine/Threonine Kinases 1, 2, and 3 (*AKT1/2/3*), and Extracellular signal-Regulated Kinase 1 and 2 (*ERK1/2*) are related to *STX4* and *TSC2* in the autophagy pathway (Cicirò & Sala, 2021). As *CTNNB1* was a common essential gene in these cells, we also examined 162 direct and functional downstream target genes of the Wnt/β-catenin pathway, as determined by down-regulation in microarray analysis following treatment by siRNA and by displaying *CTNNB1* binding peaks within ±20 kb from the transcription start site (Watanabe et al., 2014). This selection of overlapping essential genes gave us a framework to propose genetic dependencies in *POLE*-mutated MSS cancers. The selection ties together all but one of our representative cell lines, SNU-1040. This could be due to the lack of information on the DepMap website regarding this cell line's genetic dependencies and therefore needing to rely on drug sensitivities to determine which pathways are significantly relied upon.

The genetic dependencies in our selected cell lines tend to fall into three major categories: Transcription factors, autophagy, and cell survival. The pathways and the functions of these genes that these selected cell lines rely upon are discussed in this section while the possible targeting of these genetic dependencies are investigated in the Future Research Directions section. The transcription factor genes that are consistently relied upon are the Wnt and MYB family transcription factors, with the Wnt/β-catenin pathway being essential in our cell lines. This pathway has many downstream targets and is involved in cell proliferation, cell cycle dysregulation, the Warburg effect, and inflammation (Lecarpentier et al., 2019). Additionally, the Wnt/β-catenin pathway has

been recently indicated to play a role in the DDR pathway (Kaur et al. 2021). Inhibition of Wnt signaling in cancers that are genetically dependent on the gene was shown to result in BRCA-ness as indicated by a sensitivity to PARP inhibitors, as well as a decreased expression of DNA repair factors such as BRCA1, BRCA2, and FA pathway genes, identifying Wnt and/or associated factors as additional predicted hits in our DDR KO screen. The MYB family of genes *MYB* and *MYBL2* are also seen to be consistently relied upon, either directly or through their downstream targets *PLK1* and *BIRC5*. This is another family of transcription factors that have a wide array of functions in cell survival, proliferation, differentiation, and metastasis in cancer cells (Ramsay & Gonda, 2008; Srivastava et al., 2015).

For the autophagy pathway, the genes *STX4*, *TSC2*, and *NMT1* are found to be relied upon, as well as *JAK3*, *AKT1/2/3* and *ERK1/2* for autophagy signaling. STX4 is responsible for the binding of vesicles to the cell membrane and has been shown to have a critical role in the secretory autophagy process by enabling fusion of the autophagosome with the cell membrane and enabling secretion of interleukins (Kimura et al., 2017). TSC2 is known to regulate mTOR, a protein that inhibits the autophagy process (Inoki et al., 2002; Levine & Kroemer, 2019). This suggests that the autophagy process is relied upon in these cell lines, and autophagy is indeed often observed in the carcinogenesis of CRCs (Burada et al., 2015). NMT1 is known to target BID to the mitochondria and begin the process of cell death by the release of cytochrome c, but it has also been shown to modify roughly 70 proteins by N-myristoylation (Thinon et al., 2014; Zha et al., 2000).

In the cell survival pathway, the genes *BCL2L1*, *PLK1*, and *BIRC5* are relied upon in our cell lines. *BCL2L1* is an anti-apoptotic gene transcribing BCL-XL that is

downstream of transcription factors in the STAT family, functioning to inhibit proapoptotic factors BAX and BAK from initiating apoptosis (Youle & Strasser, 2008). Recent studies show that this gene is commonly relied upon as an anti-apoptotic factor in CRC, and indicates it as possibly the only BCL-2 protein overexpressed in CRCs (Scherr et al., 2020). PLK1 has been suggested to be highly expressed in many cancers, and has been shown to inhibit p53 by direct binding and phosphorylation, making it a critical gene for cell survival and cell cycle regulation (Ando et al., 2004). BIRC5, also known as survivin, is critical for the regulation of mitosis, apoptosis, and the cellular stress response and as its name suggests, prevents apoptosis and autophagic cell death (F. Li et al., 2019; Wheatley & Altieri, 2019). These genetic dependencies in late-stage *POLE*$^{P286R/+}$ cancer cells warrant further research, as they may play a role in the transformation of cells with a hypermutational Pol ε and be viable targets in the therapeutic treatment of *POLE*$^{P286R/+}$ CRC.

Study Limitations

While this study seeks to examine the DDR pathway relied upon in *POLE*$^{P286R/+}$ cells, it overlooks multiple factors involved in the observed *POLE*$^{P286R/+}$ mutation in a host. The DDR focused KO screen we would grant an understanding of the genes essential in cells that had recently undergone the *POLE*^{P286R} mutation rather than cells that had been experiencing the effects of hypermutational Pol ε for years or even decades. This can be indicated by the differing sensitivity to ATRi when comparing our generated clones to late-stage cancer cell lines. Cells with a genome that had been replicated multiple times by an erroneous Pol may also have other genetic dependencies, as a large window of time

between the *POLE* mutation and the development of cancer has been observed (Hodel et al., 2018).

Another limiting aspect of this study is the importance of the neoantigens being produced by cells expressing hypermutational Pol ε. There is undoubtedly a dependency on keeping neoantigen presentation low in cells with *POLE* mutations, but this study would only be investigating the DDR pathway that these cells rely on rather than the methods by which these cells escape the immune response (Howitt et al., 2015). Thus, this study is limited by the model that we are using. Recently, mouse models expressing $POLE^{P286R/+}$ mutations have been created, allowing the investigation of $POLE^{P286R/+}$ mutations in the context of a host organism, allowing investigation of neoantigen presentation (H.-D. Li et al., 2020).

Future Research Directions

Firstly, the next step in furthering this research would be to finish the sequencing and algorithmic sorting of the KO screen results, then following up on those results with the inhibition of those genetic dependencies to determine cell sensitivities of our $POLE^{P286R/+}$ models to ATR inhibition. Another avenue of research would be to determine sensitivity to increasing fork speed by means of PARP inhibition and determine sensitivity of our $POLE^{P286R/+}$ model to PARP inhibition, as fiber assays indicate PARP as a possible synthetic lethal target in $POLE^{P286R/+}$ cells. We may be able to determine if there are different genetic dependencies or sensitivities of $POLE^{P286R/+}$ cells that have been replicated multiple times by passaging our cell lines and performing the KO screen on a high-passage cell line, then investigating the mutational burden and mutation signature of those cells to determine their accuracy in modeling tumors with *POLE* mutations. Thirdly,

dependence on immune system escape mechanisms is often observed in tumors with *POLE* mutations, however, our model cannot undergo negative selection for neoantigen presentation by the host immune system. Hence, future research by the use of murine model systems may be helpful to look into the timelines and rates at which neoantigen presentation is present in $POLE^{P286R/+}$ cells and pathways relied upon to avoid immune detection as cells undergo replication with the hypermutational Pol ε. Also, while we did attempt a siRNA treatment targeting FANCM in both our isogenic controls and our mutant cell line, the results were indeterminate, as the treatment was equally lethal in both cell lines. While this may not bode well for the targeting of FANCM in the knockout screen, the final sequencing of the guide may still show a slight but significant decrease in the presence of the FANCM targeting guide in the $POLE^{P286R/+}$ cell line. Due to the intrinsic dependence on FANCM in U2OS, the conditions of this experiment require careful optimization in future attempts. Beyond these options for future research, there is also the investigation of targeting genetic dependencies of late-stage $POLE^{P286R/+}$ CRC identified by the DepMap and GDSC databases.

Treatment Options for Genetic Dependencies

There are many avenues that can be explored to target the genetic dependencies identified in this study. From the first part of the research suggesting genetic dependencies in the DDR pathway, we have the MMR and FA pathways, with these genes being critical earlier in *POLE*-mutated cells. A role of FANCM in Alternative Lengthening of Telomeres (ALT) has also been identified, and targeting of this pathway by FANCM inhibition is currently being investigated (O'Rourke et al., 2019). FANCM inhibitors being investigated prevent the interaction between FANCM and the RecQ-Mediated genome

Instability (RMI) complex, but this is mainly focused on inhibiting ALT, resulting in chromosomal instability (Deans & West, 2009; Voter et al., 2016). Further work would needed to determine if blocking FANCM interaction with the RMI complex is sufficient to act in a synthetically lethal manner in on *POLE*$^{P286R/+}$ cells, as recent reports indicate that the FA complex can be recruited by FANCM independently of the RMI-mediated complex (Lu et al., 2019).

Reliance on the MMR pathway also has interesting implications for treatment. Defects in the MMR pathway induce resistance to typical cytotoxic agents such as 5-FU, indicating it as possibly a poor treatment (Martin et al., 2010). Further studies show that MMR plays a critical role in the suppression of the hypermutational phenotype seen in heterozygous exonuclease deficient *POLE* cells, with an inactive MMR pathway resulting in a mutational explosion in these cells (Hodel et al., 2018). These researchers go on to argue that without the loss of the MMR pathway, heterozygous exonuclease deficient *POLE* cells are unable to attain the hypermutator phenotype seen in tumors, even though there have been MSS tumors shown with *POLE* mutations that are hypermutational (Park & Pursell, 2019). Nevertheless, there is trepidation in targeting the MMR pathway due to the resulting increased resistance to typical treatments. However, it has been shown that *POLE* exonuclease mutations can occur sporadically, often in MMR proficient hosts, and act as drivers of downstream mutations (Hu et al., 2021). Prior to this small population of somatic *POLE* mutants developing into cancer, the MMR pathway may be targeted in conjunction with Programmed cell Death protein 1 (PD1) inhibitors to have an early eradication of hypermutational *POLE*$^{P286R/+}$ cells, as it is known that a high mutational burden results in multiple neoantigens available for immune cell targeting (Nebot-Bral et

al., 2017). Genotyping of early polyps to determine somatic *POLE* mutations as well as more research to identify well-tolerated MMR targeting therapies would be required to accurately target and kill $POLE^{P286R/+}$ cells.

Our work indicates that there is also the possibility of targeting ATR early in $POLE^{P286R/+}$ tumor development. As both FANCM and the MMR pathways rely on ATR, it makes an attractive target for cells that rely on these pathways. Indeed, our generated $POLE^{P286R/+}$ cell lines showed increased sensitivity to ATRi, suggesting that ATR is critical to resolve genomic stress caused by erroneous Pol ε in these cells. The interaction of FANCM and ATR indicates that ATR inhibition may affect the functions of FANCM in fork stability and/or ICL repair. In $POLE^{P286R/+}$ cells that depend on FANCM for its role in DDR, reducing its efficiency by means of ATR inhibition may be sufficient for synthetic lethality. Beyond the FA pathway, the reduced effectiveness of the MMR pathway by deactivation of ATR may cause the hypermutation seen in cells where both MMR and Pol ε are defective, and early on in tumor development this may be a sufficient mechanism to induce cytotoxic levels of mutational burden. Moreover, any precancerous $POLE^{P286R/+}$ cells that survive the high mutational burden can be targeted by PD1 inhibitors, which would allow $POLE^{P286R/+}$ cells expressing high levels of neoantigens to be targeted by cytotoxic T cells. Meanwhile, cells proficient in MMR will not experience this high mutational burden. Therefore, ATR and PD1 inhibition may serve as an effective treatment for early cancers with somatic mutations in *POLE*.

Both of the previous targets rely on the *POLE*-deficient cells to be early on in cancer development or even pre-cancerous. However, cancer cells mutate multiple pathways beyond DDR to survive and thrive in the host environment, as indicated by the genetic

dependencies found for *POLE*-deficient MSS CRC and EC cell lines. As discussed earlier, transcription factors such as the Wnt/β-catenin pathway and MYB activation are consistently relied upon in our cell lines. Transcription factors often suggest other genetic dependencies in a tumor, but they have frequently been found to be poor and undruggable therapeutic targets. However, there have recently been trials attempting to target these genes. For instance, a DNA fusion vaccine was recently used to test MYB as a potential antigen for immune targeting in CRC (Williams et al., 2008). A more recently discovered target for MYB reliant tumors is ATR, as it is a targetable protein downstream of MYB expression (Andersson et al., 2020). Although the cell lines that we are investigating don't have significant sensitivity to ATR inhibition, this research along with studies indicating Wnt signaling as an up-regulator of DDR genes such as BRCA1, BRCA2, and FA genes suggests possible overlap between our generated models and these late stage cells' genetic dependencies (Kaur et al. 2021). Interestingly, the diabetes treatment metformin has recently been indicated as a treatment for CRC via inhibition of the Wnt/β-catenin pathway. The drug mainly operates by increasing the activity of AMPK and inhibiting mTOR, modulating many downstream pathways that CRCs rely on (Kamarudin et al., 2019). In terms of the Wnt/β-catenin pathway, metformin was found to reduce stemness and expression of Wnt in HCT115 CRC cells, which was rescued by reactivation of the pathway (Zhang & Wang, 2019). While the Wnt pathway has historically been difficult to treat, advances in the serendipitously discovered metformin treatment of CRCs have made it a safe, effective, and attractive option for the treatment of tumors dependent on the MYB pathway. Consistent with our research, *POLE*-deficient cells that rely on Wnt signaling

may also be sensitive to PARPi, indicating additional routes of treatment when treating *WNT* of *CTNNB1* genetic dependencies.

Another frequently relied upon pathway that has potential for targeting is the autophagy pathway. Recently, an unexpected and essential role for NMT1 in promoting lysosomal metabolic functions such as the enzymatic degradation of vesicle cargo and the activation of mTORC1 was identified (Chen et al., 2020). Researchers showed that inhibition of NMT1 in cancer cells resulted in reduced lysosome function and reduced mTORC1 activity, suggesting pharmacological targeting of NMT1 as a possible treatment for autophagy dependent tumors. *JAK3* and *ERK1/2*, two critical genes in our cell lines as indicated by inhibitor treatments, play a role in the autophagy signaling via the JAK-STAT pathway and the RAS pathway, respectively (Levy et al., 2017; Martinez-Lopez et al., 2013). Interestingly, the drug used to target JAK3, WHI-P97, had no targeting of JAK1/2, and JAK3 is typically only expressed in immature and differentiating hematopoietic cells (Rane & Reddy, 1994; Sudbeck et al., 1999). Rather than considering this an aberrant signaling in an already mutated cancer cell line, we will attribute this to the reliance that CRC has on the autophagy pathway, as indicated by the other genetic dependencies. Clinical trials to find safe and effective treatments that target the autophagy pathway are ongoing, and hydroxychloroquine (HQC) was recently suggested as an effective inhibitor of autophagy (Onorati et al., 2018). Inhibition of mTOR by temsirolimus increases this sensitization, indicating that this pathway may be targetable by therapies (Lee et al., 2015).

In a recent paper however, the reviewers debate if autophagy targeting is ultimately beneficial over other therapies, and the opinions are mixed (Levy et al., 2017). Targeting autophagy by reducing the effectiveness of cytokine signaling frequently results

in the suppression of the immune system, which would ultimately reduce the efficiency of the therapy (Picard et al., 2020). Therefore, targeting of the autophagy pathway directly is a fairly unattractive option for *POLE*$^{P286R/+}$ cells. However, downstream of this pathway is the cell survival pathway, which contains many genes that our studied cell lines are dependent on. BCL-XL is indicated as the only protein overexpressed in *BCL2L1* reliant CRCs, identifying it as an attractive target for treatment, and initial studies indeed implicate BCL-XL inhibitor WEHI-539 as an effective treatment for many CRC cell lines, as well as many other tumors that rely on BCL-XL as a survival factor (Kehr & Vogler, 2021; Scherr et al., 2020). Multiple inhibitors of PLK1 are currently being tested in clinical trials, as dysregulation of this pathway is common in cancers of multiple tissues but not heavily depended on in normal cells (Z. Liu et al., 2016). Cancer cells also heavily on *BIRC5*, allowing it to be safely targeted without damage to the host cells. But unfortunately, many phase II trials indicate low response to the treatments (Altieri, 2013). WEHI-539 is a novel inhibitor of BCL-XL that results in sensitization of CRCs to combination therapies. A-1331852 also functions by the same mechanism but shows higher bioavailability (Kehr & Vogler, 2021). With BCL-XL being downstream of the Jak-STAT pathway commonly utilized in autophagy signaling, targeting this protein is an excellent way to combat the autophagy commonly seen in CRCs. Other cell survival proteins such as PLK1 and survivin have been researched with less success, with survivin targeting research ongoing for decades without a clinical breakthrough due to the complexity in signaling pathways, among other complications (F. Li et al., 2019). PLK1 targeting in cancers has also been ongoing for decades with limited success, as trials have only been showing responses to the treatment when also toxic to patients (Elsayed & Wang, 2019). This would indicate

many avenues for treatment of late-stage *POLE*$^{P286R/+}$ tumors that have differing genetic dependencies when compared to early-stage or precancerous *POLE*$^{P286R/+}$ cells.

Conclusion

The final outcome of our DDR-focused screen are still pending, however completion of these studies in the future will be critical towards developing a better understanding of DNA repair dynamics in the context of replication stress caused by hypermutational Pol ε. Nonetheless, with previous work from the Lawrence lab indicating genetic dependencies in MMS *POLE* mutant cells and sensitivities determined by cell viability and fiber assays, this research supports our initial prediction that cells with *POLE*$^{P286R/+}$ mutations rely on ATR to manage replication stress, likely through the FA or MMR pathways. This research also indicates that PARP inhibition may possibly increase the fork speed of *POLE*$^{P286R/+}$ cells, and as previous research indicates that an increase in replication fork speed may be a source of genomic stress, it will be interesting to test the sensitivity to PARP inhibition in our model. With ATR, PARP, and FANCM being factors stabilizing the replication fork and *POLE*$^{P286R/+}$ indicated to have hyperactive and erroneous replication, the summation of this work shows that factors regulating replication fork stability are attractive targets in the early stages of cancers with *POLE* mutations.

Appendix 1.

Genes Targeted by KO Library

Pathway	Brief Pathway Summary	Genes to be Targeted by gRNAs
Activation of ATR	ATR functions to recognize single strand breaks and stressed replication forks, as well as R-loops. Disruption in this pathway may cause reduced single strand break recognition and stalled fork stabilization leading to increased double strand breaks or reversed forks.	RPA1
		RPA3
		RPA2
		ATRIP
		ATR
		RFC2
		RAD17
		RCF5
		RCF4
		CLSPN
		CHEK1
		HUS1
		RAD9A
		RAD17
		DBF4
		CDC7
		ORC2
		ORC6
		ORC1
		CDC6
		MCM3
		MCM2
		CDC45
Recruitment and ATM-mediated phosphorylation of repair and signaling proteins at DNA double strand breaks	ATM functions to recognize double-strand breaks. Disruption in this pathway may result in poor double strand break resolution and increased chromosomal damage.	BRCC3
		UIMC1
		ABRAXAS1
		BARD1
		BRCA1
		PIAS4
		RNF168
		HERC2

		SUMO1
		RNF8
		UBE2V2
		UBE2N
		H2AFX
		MDC1
		TPB531
		ABL1
		CHEK2
		SMARCA5
		BAZ1B
Fanconi Anemia Pathway	The Fanconi Anemia Pathway functions to resolve interstrand crosslinks and plays a role in R-loop resolution. Disruption in this pathway may cause deleterious effects to the cell's resolution of reversed forks and cause an increase in double-strand breaks.	FANCL
		WDR48
		CENPS
		CENPX
		FANCC
		FANCM
		FAAP24
		FANCD2
		FANCE
		POLN
		FANCI
		ERCC4
		FANCG
		SLX1A
		SLX4
		EME2
		MUS81
		EME1
		FANCA
		FANCF
		FAAP20
		RPA1
		RPA3
		RPA2
		ATRIP
		ATR
		DCLRE1B
		DCLRE1A
		FAN1
Homology Directed Repair	Homology Directed Repair uses the sister chromatid as a template to resolve double-strand breaks and is the most accurate double strand	PTOPB1
		BRIP1
		HUS1

	break repair mechanism. Disruption in this pathway may cause the cell to rely on less accurate non-homologous end joining to repair double strand breaks.	RADA91
		RAD17
		DNA2
		BLM
		TOP3A
		RMI2
		RMI1
		WRN
		EXO1
		ATRIP
		ATR
		RPA3
		RPA2
		RPA1
		ATM
		NBN
		MRE11
		RAD50
		KAT5
		BARD1
		RBBP8
		RAD51C
		BRCA2
		LIG3
		XRCC1
		RFC1
		PCNA
		POLE
		POLD3
		POLD4
		POLK
		POLH
		ABL1
		RAD51AP1
		PALB2
		RAD51
		XRCC2
		XRCC3
		BABAM1
		BABAM2
		BRCC3
		UIMC1
		ABRAXAS1

		PIAS4
		RNF168
		HERC2
		SUMO1
		RNF8
		UBE2V2
		UBE2N
		H2AFX
		MDC1
		TP53BP1
		SLX1A
		SLX4
		SPIDR
		SIRT6
		ERCC4
		ERCC1
		CHEK1
		EME2
		MUS81
		EME1
		PARP2
		PARP1
		GEN1
		FEN1
		SUMO2
		POLQ
		CLSPN
		RTEL1
Base Excision Repair	Base Excision Repair functions to remove damaged bases prior to replication in order to reduce fork stalling or misincorporation of nucleotides during the replication process. Disruptions in the pathway may cause increased fork stalling or a higher nucleotide misincorporation rate.	NEIL2
		UNG
		APEX1
		POLB
		LIG3
		XRCC1
		LIG1
		NEIL1
		MUTYH
		RFC2
		RFC1
		RFC5
		RFC4
		RFC3
		PCNA

		POLE
		POLD1
		POLD3
		POLD4
		RPA1
		RPA3
		RPA2
		OGG1
		FEN1
		PARP2
		PARP1
		MBD4
		SMUG1
Non-Homologous End Joining	Non-Homologous End Joining functions as the most common and less accurate type of double strand break resolution. Disruptions in this pathway may lead to high mutational burden and difficulty in resolving many DNA damage types.	XRCC6
		XRCC5
		PRKDC
		DCLRE1C
		MDC1
		BABAM1
		BABAM2
		BRCC3
		BARD1
		BRCA1
		UIMC1
		ABRAXAS1
		PIAS4
		RNF168
		HERC2
		SUMO1
		RNF8
		UBE2V2
		UBE2N
		H2AFX
		ATM
		KAT5
		NBN
		MRE11
		RAD50
		TP53BP1
		PAXIP1
		POLM
		POLL
		XRCC4

		LIG4
		TDP1
		RIF1
Microhomology-Mediated End Joining Alt-NHEJ	Microhomology-Mediated End Joining is a less common and the least accurate form of end joining that functions to generate small portions of homology to resolve double strand breaks. Disruptions in this pathway may increase reliance on other double strand break repair pathways.	LIG3
		XRCC1
		MRE11
		RAD50
		NBN
		RBBP8
		FEN1
		PARP2
		PARP1
		POLQ
Mismatch Repair	Mismatch Repair functions to recognize, remove, and correct misincorporated nucleotides. Disruptions in this pathway may lead to increased mutational burden and decreased replication fidelity.	PCNA
		MSH2
		MSH3
		MSH6
		MLH1
		PMS2
		LIG1
		EXO1
		RPA1
		RPA3
		RPA2
		POLD1
		POLD3
		POLD4
DNA Damage Reversal	DNA Damage Reversal functions to directly reverse DNA damage such as alkylating agents or UV damage. Disruptions in this pathway may cause less accurate resolutions of these types of damage.	ALKBH2
		ASCC2
		ASCC3
		ASCC1
		ALKBH3
		MGMT
		ALKBH5
		FTO
Cell Cycle Checkpoints	Cell Cycle Checkpoints function to regulate the passage of the cell from one step of the cell cycle to the next based on, among other things, genomic stress. Disruption in this pathway may cause reduced apoptosis in response to genomic stress or increased mutational burden.	TP53
		BABAM1
		BABAM2
		BRCC3
		UIMC1
		ABRAXAS1
		BARD1
		BRCA1

		PIAS4
		RNF168
		HERC2
		SUMO1
		RNF8
		UBE2V2
		UBE2N
		H2AFX
		ATM
		KAT5
		NBN
		MRE11
		RAD50
		MDC1
		TP53BP1
		RPA1
		RPA3
		RPA2
		ATRIP
		ATR
		CDKN1A
		RFC2
		RAD17
		RFC5
		RFC4
		RFC3
		CLSPN
		XPO1
		NUP98
		NUP107
		NUP160
		NUP133
		CENPS
		DYNLL1
		CHEK2
		CHEK1
		HUS1
		RAD9A
		RAD17
		SEM1
		DBF4
		CDC7
		ORC2

		ORC6
		ORC1
		CDC6
		MCM3
		MCM2
		CDC45
		RHNO1
		TOPB1
		BRIP1
		DNA2
		BLM
		TOP3A
		WRN
		EXO1
		RBBP8
DNA Replication	DNA Replication functions to elongate a daughter DNA strand using a parental template strand. Disruption in this pathway may cause decreased fork stability or increased mutational burden.	POLE
		PCNA
		ORC2
		ORC6
		ORC1
		CDC6
		MCM3
		POLD1
		POLD4
		PRIM1
		POLA1
		POLA2
		PRIM2
		RPA1
		RPA3
		RPA2
		RFC2
		RFC1
		RFC5
		RFC4
		RFC3
		DNA2
		GINS2
		LIG1
		GMNN
		GINS1
		DBF4
		CDC7

		CDC45
		RPA4
		FEN1
		GINS3
		SEM1
		GINS4
RNA Pol II Transcription Elongation	RNA Pol II Transcription Elongation functions to facilitate the transcription of RNA using DNA as a template after the transcription has been initiated. Disruption in this pathway may cause an increase in R-loops, errors in RNA splicing, and replication stress by RNA Pol II stalling.	GTF2H4
		ERCC3
		CDK7
		ERCC2
		POLR2A
		SUPT16H
		TCEA1
		ELOC
		NELFE
		NELFB
		SUPT4H1
		SUPT5H
		RTF1
		CDC73
		LEO1
		WDR61
		IWS1
mRNA Splicing-Major Pathway	The mRNA Splicing Pathway functions to remove introns from RNA that codes for proteins. Disruption in this pathway may cause increased R-loops or erroneous translation.	AQR
		ALYREF
		FUS
		PPIE
		CPSF4
		SYMPK
		CPSF2
		WDR33
		NUDT21
		XAB2
		CDC5L
		PRPF19
		RBM17
		HNRNPF
		RBNX
		HNRNPK
		HNRNPM
		HNRNPR
		HNRNPU
		PTBP1

		DDX5
		HNRNPA1
		HNRNPA2B1
		HNRNPA2B1
		HNRNPC
		HNRNPD
		DHX9
		MAGOH
		POLR2A
		SLU7
mRNA 3'-end Processing	mRNA 3'-end Processing functions to polyadenylate the 3'-end of mRNA for effective transport out of the nuclear envelope. Disruptions in this process may lead to a lack of transport out of the nucleus, an increase in R-loops, and difficulty in protein production.	ALYREF
		CPSF4
		SYMPK
		CPSF2
		WDR33
		NUDT21
		MAGOH
		POLDIP3
		SLU7
		DDX39A
		THOC5
		THOC2
		THOC6
Transport of Mature mRNA Derived from an Intron-Containing Transcript	The Transport of Mature mRNAs Derived from Intron-Containing Transcripts functions to transport mRNA out of the nuclear envelope after the mRNA has undergone splicing. Disruptions in this process may lead to a lack of transport out of the nucleus, an increase in R-loops, and difficulty in protein production.	NUP43
		NUP160
		NUP37
		NUP85
		NUP133
		SEC13
		TPR
		NUP153
		NUP88
		NUP188
		NUP214
		NDC1
		NUP205
		NUP155
		NUP210
		NUP93
		POM121
		POM121C
		NUP35
		SEH1L

		RAE1
		NUP98
		NUP62
		NUP58
		NUP50
		AAAS
		RANBP2
		NUPL2
		SLU7
		DDX39B
		DDX39A
		FYTTD1
		LUZP4
		SARNP
		GEL1
		ZCH11A
		CHTOP
		THOC5
		THOC3
		THOC2
		THOC1
		THOC7
		THOC6
Chromatin Organization	Chromatin Organization functions to regulate the expression of genes based on the structure of the chromatin, increasing or decreasing expression as necessary. Disruption in this process may cause erroneous gene expression or chromatin instability.	ARID1A
		SUV39H1
		KAT7
		ACTL6A
		H2AFX
		SMARCA2
		SMARCA4
		RBBP4
		SPARCB1
		CHD3
		HDAC1
		CHD4
		SETB1
		RBBP7
		CARM1
		ARID1B
		ING5
		HDAC2
		KAT2A
		KAT2B

		KAT5
		SETD2
		SAP130
		ENY2
		DMAP1
		RUVBL2
		RUVBL1
DNA Damage Bypass	DNA Damage Bypass or translesion synthesis functions to resolve DNA stress by having error-prone DNA polymerases replicate DNA across a lesion on the template strand. Disruption in this pathway may lead to increased replication stress and fork stalling.	VCP
		UFD1
		NPLOC4
		RFC2
		RFC1
		RFC5
		RFC4
		RFC3
		RPA1
		RPA3
		RPA2
		PCNA
		UBC
		UBB
		UBA52
		RPS27A
		POLH
		SPRTN
		WDR48
		USP1
		POLE2
		POLE
		POL3
		POL4
		POLD1
		POLD2
		POLD3
		POLD4
		ZBTB32
		RCHY1
		ISG15
		POLI
		POLK
		REV1
		DDB1
		RBX1

		CUL4A
		CUL4B
		DTL
		RAD18
		UBE2B
		MAD2L2
		REV3L
		USP10
		UBA7
		USP43
		PCLAF
		UBE2L6
		TRIM25

Table 2. Genes Targeted by KO Library

This table contains the genes that were targeted by the KO library, sorted by the associated pathway these genes function in and given a brief description of the logic behind targeting of that pathway.

gRNA and ssODN Sequences for *POLE*^{P286R} Knock-in

- Guide sequence: UCUCAGCAUCAGGAAACUUG, sourced from Synthego
- ssODN sequence:

  GGCATTTGACATTGAGACGACCAAACTGCCtCTCAAGTTTCgTGATGCT

  GAGACAGACCAGATTATGATGATTTCCTACATGATCGATGGCCAGGTG

  AGCAGGTGGCTTCTGGGAAGTAAGCTCCTG, sourced from IDT

Additional Fiber Assay Results

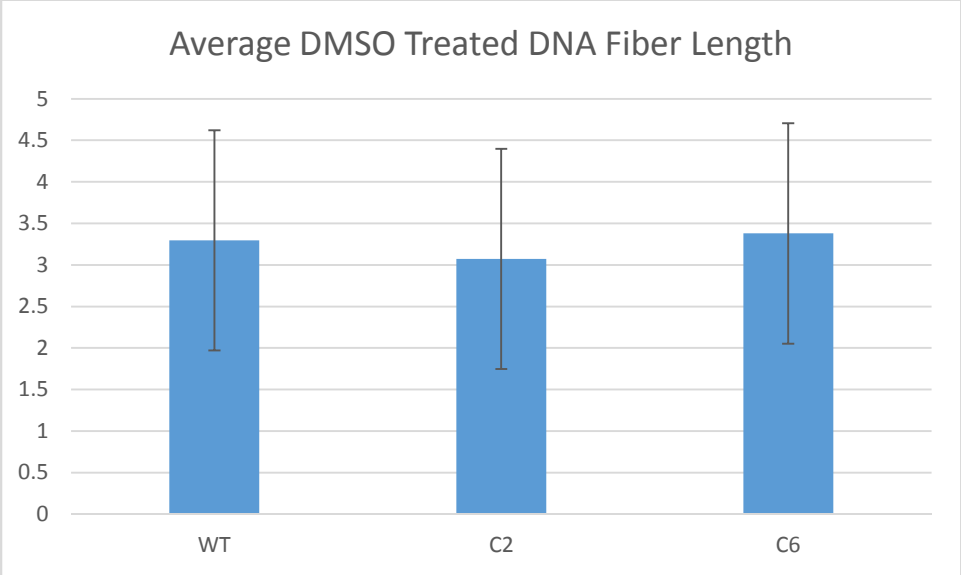


Figure 14.Average DMSO Treated Fiber Length

Average length of each cell line's DNA fibers when treated with DMSO, with error bars representing one standard deviation.

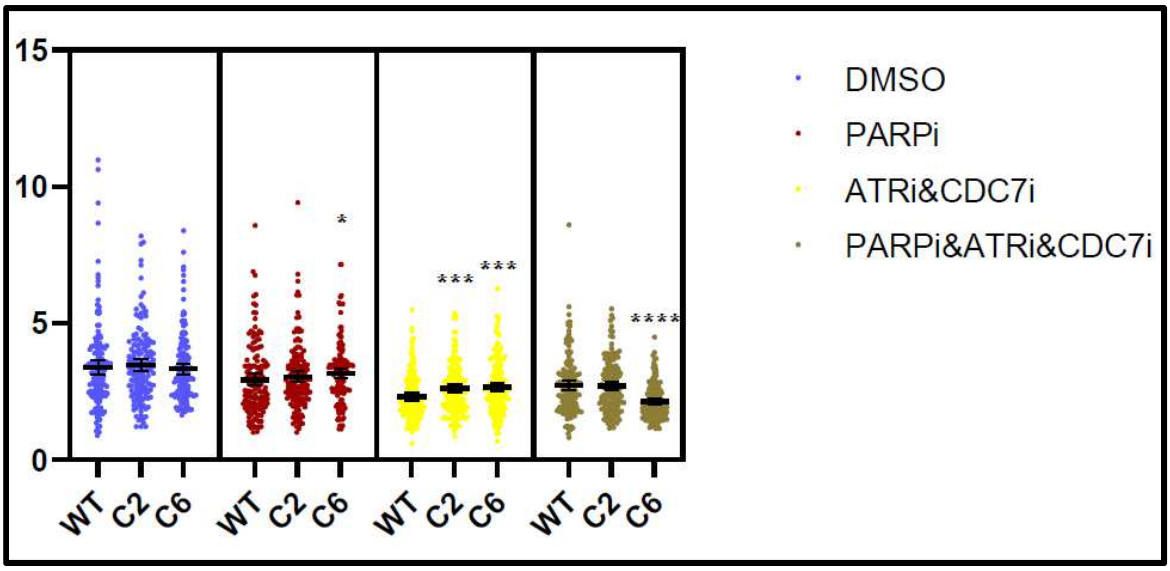


Figure 15.Additional Fiber Assay Results

*Conditions for previous fiber assay were repeated. At least 150 fibers were measured for each cell line in each condition. Lines represent the median value of the cell line's IdU:CldU ratio. *: $p<0.05$, ***: $p<0.001$ ****: $p<0.0001$ as assessed by a two-sided Mann-Whitney statistical analysis of median values.*

References

Lentiviral sources:

psPAX2 was a gift from Didier Trono (Addgene plasmid # 12260 ; http://n2t.net/addgene:12260 ; RRID:Addgene_12260)

pCI-VSVG was a gift from Garry Nolan (Addgene plasmid # 1733 ; http://n2t.net/addgene:1733 ; RRID:Addgene_1733)

Alexandrov, L. B., Ju, Y. S., Haase, K., Van Loo, P., Martincorena, I., Nik-Zainal, S., Totoki, Y., Fujimoto, A., Nakagawa, H., Shibata, T., Campbell, P. J., Vineis, P., Phillips, D. H., & Stratton, M. R. (2016). Mutational signatures associated with tobacco smoking in human cancer. *Science (New York, N.Y.)*, *354*(6312), 618–622. https://doi.org/10.1126/science.aag0299

Alexandrov, L. B., Kim, J., Haradhvala, N. J., Huang, M. N., Tian Ng, A. W., Wu, Y., Boot, A., Covington, K. R., Gordenin, D. A., Bergstrom, E. N., Islam, S. M. A., Lopez-Bigas, N., Klimczak, L. J., McPherson, J. R., Morganella, S., Sabarinathan, R., Wheeler, D. A., Mustonen, V., Getz, G., … Stratton, M. R. (2020). The repertoire of mutational signatures in human cancer. *Nature*, *578*(7793), 94–101. https://doi.org/10.1038/s41586-020-1943-3

Altieri, D. C. (2013). Targeting survivin in cancer. *Cancer Letters*, *332*(2), 225–228. https://doi.org/10.1016/j.canlet.2012.03.005

Andersson, M. K., Mangiapane, G., Nevado, P. T., Tsakaneli, A., Carlsson, T., Corda, G., Nieddu, V., Abrahamian, C., Chayka, O., Rai, L., Wick, M., Kedaigle, A., Stenman, G., & Sala, A. (2020). ATR is a MYB regulated gene and potential therapeutic target in adenoid cystic carcinoma. *Oncogenesis*, *9*(1), 1–10. https://doi.org/10.1038/s41389-020-0194-3

Ando, K., Ozaki, T., Yamamoto, H., Furuya, K., Hosoda, M., Hayashi, S., Fukuzawa, M., & Nakagawara, A. (2004). Polo-like kinase 1 (Plk1) inhibits p53 function by physical interaction and phosphorylation. *The Journal of Biological Chemistry*, *279*(24), 25549–25561. https://doi.org/10.1074/jbc.M314182200

Barbari, S. R., Kane, D. P., Moore, E. A., & Shcherbakova, P. V. (2018). Functional Analysis of Cancer-Associated DNA Polymerase ε Variants in Saccharomyces cerevisiae. *G3 Genes|Genomes|Genetics*, *8*(3), 1019–1029. https://doi.org/10.1534/g3.118.200042

Basbous, J., & Constantinou, A. (2019). A tumor suppressive DNA translocase named FANCM. *Critical Reviews in Biochemistry & Molecular Biology*, *54*(1), 27–40. https://doi.org/10.1080/10409238.2019.1568963

Boland, C. R., & Goel, A. (2010). Microsatellite Instability in Colorectal Cancer. *Gastroenterology*, *138*(6), 2073-2087.e3. https://doi.org/10.1053/j.gastro.2009.12.064

Bourdais, R., Rousseau, B., Pujals, A., Boussion, H., Joly, C., Guillemin, A., Baumgaertner, I., Neuzillet, C., & Tournigand, C. (2017). Polymerase proofreading domain mutations: New opportunities for immunotherapy in hypermutated colorectal cancer beyond MMR deficiency. *Critical Reviews in Oncology/Hematology*, *113*, 242–248. https://doi.org/10.1016/j.critrevonc.2017.03.027

Briggs, S., & Tomlinson, I. (2013). Germline and somatic polymerase ϵ and δ mutations define a new class of hypermutated colorectal and endometrial cancers. *The Journal of Pathology*, *230*(2), 148–153. https://doi.org/10.1002/path.4185

Burada, F., Nicoli, E. R., Ciurea, M. E., Uscatu, D. C., Ioana, M., & Gheonea, D. I. (2015). Autophagy in colorectal cancer: An important switch from physiology to pathology. *World Journal of Gastrointestinal Oncology*, *7*(11), 271–284. https://doi.org/10.4251/wjgo.v7.i11.271

Burgers, P. M. J., & Kunkel, T. A. (2017). Eukaryotic DNA Replication Fork. *Annual Review of Biochemistry*, *86*(1), 417–438. https://doi.org/10.1146/annurev-biochem-061516-044709

Campbell, B. B., Light, N., Fabrizio, D., Zatzman, M., Fuligni, F., de Borja, R., Davidson, S., Edwards, M., Elvin, J. A., Hodel, K. P., Zahurancik, W. J., Suo, Z., Lipman, T., Wimmer, K., Kratz, C. P., Bowers, D. C., Laetsch, T. W., Dunn, G. P., Johanns, T. M., … Shlien, A. (2017). Comprehensive Analysis of Hypermutation in Human Cancer. *Cell*, *171*(5), 1042-1056.e10. https://doi.org/10.1016/j.cell.2017.09.048

Carethers, J. M., & Jung, B. H. (2015). Genetics and Genetic Biomarkers in Sporadic Colorectal Cancer. *Gastroenterology*, *149*(5), 1177-1190.e3. https://doi.org/10.1053/j.gastro.2015.06.047

Castella, M., Jacquemont, C., Thompson, E. L., Yeo, J. E., Cheung, R. S., Huang, J.-W., Sobeck, A., Hendrickson, E. A., & Taniguchi, T. (2015). FANCI Regulates Recruitment of the FA Core Complex at Sites of DNA Damage Independently of FANCD2. *PLOS Genetics*, *11*(10), e1005563. https://doi.org/10.1371/journal.pgen.1005563

Chen, Y.-C., Navarrete, M. S., Wang, Y., McClintock, N. C., Sakurai, R., Wang, F., Chen, K. T., Chou, T.-F., Rehan, V. K., Lee, D. J., & Diaz, B. (2020). N-myristoyltransferase-1 is necessary for lysosomal degradation and mTORC1 activation in cancer cells. *Scientific Reports*, *10*(1), 11952. https://doi.org/10.1038/s41598-020-68615-w

Cicirò, Y., & Sala, A. (2021). MYB oncoproteins: Emerging players and potential therapeutic targets in human cancer. *Oncogenesis*, *10*(2), 1–15. https://doi.org/10.1038/s41389-021-00309-y

Deans, A. J., & West, S. C. (2009). FANCM Connects the Genome Instability Disorders Bloom's Syndrome and Fanconi Anemia. *Molecular Cell*, *36*(6), 943–953. https://doi.org/10.1016/j.molcel.2009.12.006

Doench, J. G., Fusi, N., Sullender, M., Hegde, M., Vaimberg, E. W., Donovan, K. F., Smith, I., Tothova, Z., Wilen, C., Orchard, R., Virgin, H. W., Listgarten, J., & Root, D. E. (2016). Optimized sgRNA design to maximize activity and minimize off-target effects of CRISPR-Cas9. *Nature Biotechnology*, *34*(2), 184–191. https://doi.org/10.1038/nbt.3437

Doudna, J. A., & Charpentier, E. (2014). The new frontier of genome engineering with CRISPR-Cas9. *Science*, *346*(6213), 1258096. https://doi.org/10.1126/science.1258096

Eki, T. (1994). Poly (ADP-ribose) polymerase inhibits DNA replication by human replicative DNA polymerase α, δ and ε in vitro. *FEBS Letters*, *356*(2), 261–266. https://doi.org/10.1016/0014-5793(94)01280-6

Elsayed, I., & Wang, X. (2019). PLK1 inhibition in cancer therapy: Potentials and challenges. *Future Medicinal Chemistry*, *11*(12), 1383–1386. https://doi.org/10.4155/fmc-2019-0084

Esteban-Jurado, C., Giménez-Zaragoza, D., Muñoz, J., Franch-Expósito, S., Álvarez-Barona, M., Ocaña, T., Cuatrecasas, M., Carballal, S., López-Cerón, M., Marti-Solano, M., Díaz-Gay, M., van Wezel, T., Castells, A., Bujanda, L., Balmaña, J., Gonzalo, V., Llort, G., Ruiz-Ponte, C., Cubiella, J., … Castellví-Bel, S. (2017). POLE and POLD1 screening in 155 patients with multiple polyps and early-onset colorectal cancer. *Oncotarget*, *8*(16), 26732–26743. https://doi.org/10.18632/oncotarget.15810

Fang, H., Barbour, J. A., Poulos, R. C., Katainen, R., Aaltonen, L. A., & Wong, J. W. H. (2020). Mutational processes of distinct POLE exonuclease domain mutants drive an enrichment of a specific TP53 mutation in colorectal cancer. *PLoS Genetics*, *16*(2), e1008572. https://doi.org/10.1371/journal.pgen.1008572

Flygare, J., Aspesi, A., Bailey, J. C., Miyake, K., Caffrey, J. M., Karlsson, S., & Ellis, S. R. (2006). Human RPS19, the gene mutated in Diamond-Blackfan anemia, encodes a ribosomal protein required for the maturation of 40S ribosomal subunits. *Blood*, *109*(3), 980–986. https://doi.org/10.1182/blood-2006-07-038232

Galati, M. A., Hodel, K. P., Gams, M. S., Sudhaman, S., Bridge, T., Zahurancik, W. J., Ungerleider, N. A., Park, V. S., Ercan, A. B., Joksimovic, L., Siddiqui, I., Siddaway, R., Edwards, M., Borja, R. de, Elshaer, D., Chung, J., Forster, V. J., Nunes, N. M., Aronson, M., … Tabori, U. (2020). Cancers from Novel Pole-

Mutant Mouse Models Provide Insights into Polymerase-Mediated Hypermutagenesis and Immune Checkpoint Blockade. *Cancer Research*, *80*(24), 5606–5618. https://doi.org/10.1158/0008-5472.CAN-20-0624

Garg, P., & Burgers, P. M. J. (2005). DNA Polymerases that Propagate the Eukaryotic DNA Replication Fork. *Critical Reviews in Biochemistry & Molecular Biology*, *40*(2), 115–128. https://doi.org/10.1080/10409230590935433

Guo, S., Zhang, Y., Yuan, F., Gao, Y., Gu, L., Wong, I., & Li, G.-M. (2006). Regulation of Replication Protein A Functions in DNA Mismatch Repair by Phosphorylation *. *Journal of Biological Chemistry*, *281*(31), 21607–21616. https://doi.org/10.1074/jbc.M603504200

Gupta, D., Lin, B., Cowan, A., & Heinen, C. D. (2018). ATR-Chk1 activation mitigates replication stress caused by mismatch repair-dependent processing of DNA damage. *Proceedings of the National Academy of Sciences of the United States of America*, *115*(7), 1523–1528. https://doi.org/10.1073/pnas.1720355115

Hamzaoui, N., Alarcon, F., Leulliot, N., Guimbaud, R., Buecher, B., Colas, C., Corsini, C., Nuel, G., Terris, B., Laurent-Puig, P., Chaussade, S., Dhooge, M., Madru, C., & Clauser, E. (2020). Genetic, structural, and functional characterization of POLE polymerase proofreading variants allows cancer risk prediction. *Genetics in Medicine*, *22*(9), 1533–1541. https://doi.org/10.1038/s41436-020-0828-z

Haradhvala, N. J., Kim, J., Maruvka, Y. E., Polak, P., Rosebrock, D., Livitz, D., Hess, J. M., Leshchiner, I., Kamburov, A., Mouw, K. W., Lawrence, M. S., & Getz, G. (2018). Distinct mutational signatures characterize concurrent loss of polymerase proofreading and mismatch repair. *Nature Communications*, *9*(1), 1746. https://doi.org/10.1038/s41467-018-04002-4

Hocke, S., Guo, Y., Job, A., Orth, M., Ziesch, A., Lauber, K., De Toni, E. N., Gress, T. M., Herbst, A., Göke, B., & Gallmeier, E. (2016). A synthetic lethal screen identifies ATR-inhibition as a novel therapeutic approach for POLD1-deficient cancers. *Oncotarget*, *7*(6), 7080–7095. https://doi.org/10.18632/oncotarget.6857

Hodel, K. P., de Borja, R., Henninger, E. E., Campbell, B. B., Ungerleider, N., Light, N., Wu, T., LeCompte, K. G., Goksenin, A. Y., Bunnell, B. A., Tabori, U., Shlien, A., & Pursell, Z. F. (2018). Explosive mutation accumulation triggered by heterozygous human Pol ε proofreading-deficiency is driven by suppression of mismatch repair. *ELife*, *7*, e32692. https://doi.org/10.7554/eLife.32692

Howitt, B. E., Shukla, S. A., Sholl, L. M., Ritterhouse, L. L., Watkins, J. C., Rodig, S., Stover, E., Strickland, K. C., D'Andrea, A. D., Wu, C. J., Matulonis, U. A., & Konstantinopoulos, P. A. (2015). Association of Polymerase e–Mutated and Microsatellite-Instable Endometrial Cancers With Neoantigen Load, Number of Tumor-Infiltrating Lymphocytes, and Expression of PD-1 and PD-L1. *JAMA Oncology*, *1*(9), 1319–1323. https://doi.org/10.1001/jamaoncol.2015.2151

Hu, H., Cai, W., Wu, D., Hu, W., Dong Wang, L., Mao, J., Zheng, S., & Ge, W. (2021). Ultra-mutated colorectal cancer patients with POLE driver mutations exhibit distinct clinical patterns. *Cancer Medicine*, *10*(1), 135–142. https://doi.org/10.1002/cam4.3579

Inoki, K., Li, Y., Zhu, T., Wu, J., & Guan, K.-L. (2002). TSC2 is phosphorylated and inhibited by Akt and suppresses mTOR signalling. *Nature Cell Biology*, *4*(9), 648–657. https://doi.org/10.1038/ncb839

Jain, R., Aggarwal, A. K., & Rechkoblit, O. (2018). Eukaryotic DNA polymerases. *Current Opinion in Structural Biology*, *53*, 77–87. https://doi.org/10.1016/j.sbi.2018.06.003

Joung, J., Konermann, S., Gootenberg, J. S., Abudayyeh, O. O., Platt, R. J., Brigham, M. D., Sanjana, N. E., & Zhang, F. (2017). Genome-scale CRISPR-Cas9 Knockout and Transcriptional Activation Screening. *Nature Protocols*, *12*(4), 828–863. https://doi.org/10.1038/nprot.2017.016

Kamarudin, M. N. A., Sarker, Md. M. R., Zhou, J.-R., & Parhar, I. (2019). Metformin in colorectal cancer: Molecular mechanism, preclinical and clinical aspects. *Journal of Experimental & Clinical Cancer Research*, *38*(1), 491. https://doi.org/10.1186/s13046-019-1495-2

Kaur, A., Lim, J., Sepramaniam, S., Patnaik, S., Harmston, N., Lee, M., . . . Madan, B. (2021). WNT inhibition creates a BRCA□like state in Wnt□addicted cancer. EMBO Molecular Medicine, 13(4), E13349-N/a.

Kawakami, H., Zaanan, A., & Sinicrope, F. A. (2015). Microsatellite Instability Testing and Its Role in the Management of Colorectal Cancer. *Current Treatment Options in Oncology*, *16*(7), 30. https://doi.org/10.1007/s11864-015-0348-2

Kehr, S., & Vogler, M. (2021). It's time to die: BH3 mimetics in solid tumors. *Biochimica et Biophysica Acta (BBA) - Molecular Cell Research*, *1868*(5), 118987. https://doi.org/10.1016/j.bbamcr.2021.118987

Kesti, T., Flick, K., Keränen, S., Syväoja, J. E., & Wittenberg, C. (1999). DNA Polymerase ε Catalytic Domains Are Dispensable for DNA Replication, DNA Repair, and Cell Viability. *Molecular Cell*, *3*(5), 679–685. https://doi.org/10.1016/S1097-2765(00)80361-5

Kimura, T., Jia, J., Kumar, S., Choi, S. W., Gu, Y., Mudd, M., Dupont, N., Jiang, S., Peters, R., Farzam, F., Jain, A., Lidke, K. A., Adams, C. M., Johansen, T., & Deretic, V. (2017). Dedicated SNAREs and specialized TRIM cargo receptors mediate secretory autophagy. *The EMBO Journal*, *36*(1), 42–60. https://doi.org/10.15252/embj.201695081

Kolinjivadi, A. M., Crismani, W., & Ngeow, J. (2020). Emerging functions of Fanconi anemia genes in replication fork protection pathways. *Human Molecular Genetics*, *29*(R2), R158–R164. https://doi.org/10.1093/hmg/ddaa087

Kunkel, T. A. (2009). Evolving Views of DNA Replication (In)Fidelity. *Cold Spring Harbor Symposia on Quantitative Biology*, *74*(0), 91–101. https://doi.org/10.1101/sqb.2009.74.027

Kuznetsova, A. Y., Seget, K., Moeller, G. K., de Pagter, M. S., de Roos, J. A. D. M., Dürrbaum, M., Kuffer, C., Müller, S., Zaman, G. J. R., Kloosterman, W. P., & Storchová, Z. (2015). Chromosomal instability, tolerance of mitotic errors and multidrug resistance are promoted by tetraploidization in human cells. *Cell Cycle*, *14*(17), 2810–2820. https://doi.org/10.1080/15384101.2015.1068482

Lecarpentier, Y., Schussler, O., Hébert, J.-L., & Vallée, A. (2019). Multiple Targets of the Canonical WNT/β-Catenin Signaling in Cancers. *Frontiers in Oncology*, *9*, 1248. https://doi.org/10.3389/fonc.2019.01248

Lee, H.-O., Mustafa, A., Hudes, G. R., & Kruger, W. D. (2015). Hydroxychloroquine Destabilizes Phospho-S6 in Human Renal Carcinoma Cells. *PLOS ONE*, *10*(7), e0131464. https://doi.org/10.1371/journal.pone.0131464

León-Castillo, A., Britton, H., McConechy, M. K., McAlpine, J. N., Nout, R., Kommoss, S., Brucker, S. Y., Carlson, J. W., Epstein, E., Rau, T. T., Bosse, T., Church, D. N., & Gilks, C. B. (2020). Interpretation of somatic POLE mutations in endometrial carcinoma. *The Journal of Pathology*, *250*(3), 323–335. https://doi.org/10.1002/path.5372

Levine, B., & Kroemer, G. (2019). Biological Functions of Autophagy Genes: A Disease Perspective. *Cell*, *176*(1), 11–42. https://doi.org/10.1016/j.cell.2018.09.048

Levy, J. M. M., Towers, C. G., & Thorburn, A. (2017). Targeting autophagy in cancer. *Nature Reviews Cancer*, *17*(9), 528–542. https://doi.org/10.1038/nrc.2017.53

Li, F., Aljahdali, I., & Ling, X. (2019). Cancer therapeutics using survivin BIRC5 as a target: What can we do after over two decades of study? *Journal of Experimental & Clinical Cancer Research*, *38*(1), 368. https://doi.org/10.1186/s13046-019-1362-1

Li, G.-M. (2008). Mechanisms and functions of DNA mismatch repair. *Cell Research*, *18*(1), 85–98. https://doi.org/10.1038/cr.2007.115

Li, H.-D., Cuevas, I., Zhang, M., Lu, C., Alam, M. M., Fu, Y.-X., You, M. J., Akbay, E. A., Zhang, H., & Castrillon, D. H. (2018). Polymerase-mediated ultramutagenesis in mice produces diverse cancers with high mutational load. *The Journal of Clinical Investigation*, *128*(9), 4179–4191. https://doi.org/10.1172/JCI122095

Li, H.-D., Lu, C., Zhang, H., Hu, Q., Zhang, J., Cuevas, I. C., Sahoo, S. S., Aguilar, M., Maurais, E. G., Zhang, S., Wang, X., Akbay, E. A., Li, G.-M., Li, B., Koduru, P., Ly, P., Fu, Y.-X., & Castrillon, D. H. (2020). A *Pole*^{P286R} mouse model of endometrial cancer recapitulates high mutational burden and immunotherapy response. *JCI Insight*, *5*(14). https://doi.org/10.1172/jci.insight.138829

Li, W., Xu, H., Xiao, T., Cong, L., Love, M. I., Zhang, F., Irizarry, R. A., Liu, J. S., Brown, M., & Liu, X. S. (2014). MAGeCK enables robust identification of essential genes from genome-scale CRISPR/Cas9 knockout screens. *Genome Biology*, *15*(12), 554. https://doi.org/10.1186/s13059-014-0554-4

Li, Z., Pearlman, A. H., & Hsieh, P. (2016). DNA mismatch repair and the DNA damage response. *DNA Repair*, *38*, 94–101. https://doi.org/10.1016/j.dnarep.2015.11.019

Ling, C., Huang, J., Yan, Z., Li, Y., Ohzeki, M., Ishiai, M., Xu, D., Takata, M., Seidman, M., & Wang, W. (2016). Bloom syndrome complex promotes FANCM recruitment to stalled replication forks and facilitates both repair and traverse of DNA interstrand crosslinks. *Cell Discovery*, *2*(1), 1–18. https://doi.org/10.1038/celldisc.2016.47

Liu, B., Nicolaides, N. C., Markowitz, S., Willson, J. K. V., Parsons, R. E., Jen, J., Papadopolous, N., Peltomäki, P., de la Chapelle, A., Hamilton, S. R., Kinzler, K. W., & Vogelstein, B. (1995). Mismatch repair gene defects in sporadic colorectal cancers with microsatellite instability. *Nature Genetics*, *9*(1), 48–55. https://doi.org/10.1038/ng0195-48

Liu, D., Frederiksen, J. H., Liberti, S. E., Lützen, A., Keijzers, G., Pena-Diaz, J., & Rasmussen, L. J. (2017). Human DNA polymerase delta double-mutant D316A;E318A interferes with DNA mismatch repair in vitro. *Nucleic Acids Research*, *45*(16), 9427–9440. https://doi.org/10.1093/nar/gkx611

Liu, Y., Fang, Y., Shao, H., Lindsey-Boltz, L., Sancar, A., & Modrich, P. (2010). Interactions of Human Mismatch Repair Proteins MutSα and MutLα with Proteins of the ATR-Chk1 Pathway *. *Journal of Biological Chemistry*, *285*(8), 5974–5982. https://doi.org/10.1074/jbc.M109.076109

Liu, Z., Sun, Q., & Wang, X. (2016). PLK1, A Potential Target for Cancer Therapy. *Translational Oncology*, *10*(1), 22–32. https://doi.org/10.1016/j.tranon.2016.10.003

Lopez-Martinez, D., Liang, C., & Cohn, M. (2016). Cellular response to DNA interstrand crosslinks: The Fanconi anemia pathway. Cellular and Molecular Life Sciences : CMLS, 73(16), 3097-3114.

Lu, R., O'Rourke, J. J., Sobinoff, A. P., Allen, J. A. M., Nelson, C. B., Tomlinson, C. G., Lee, M., Reddel, R. R., Deans, A. J., & Pickett, H. A. (2019). The FANCM-BLM-TOP3A-RMI complex suppresses alternative lengthening of telomeres

(ALT). *Nature Communications*, *10*(1), 2252. https://doi.org/10.1038/s41467-019-10180-6

Ma, J., Setton, J., Lee, N. Y., Riaz, N., & Powell, S. N. (2018). The therapeutic significance of mutational signatures from DNA repair deficiency in cancer. *Nature Communications*, *9*(1), 3292. https://doi.org/10.1038/s41467-018-05228-y

Maréchal, A., & Zou, L. (2013). DNA Damage Sensing by the ATM and ATR Kinases. *Cold Spring Harbor Perspectives in Biology*, *5*(9), a012716. https://doi.org/10.1101/cshperspect.a012716

Markowitz, S., Wang, J., Myeroff, L., Parsons, R., & al, et. (1995). Inactivation of the type II TGF-beta receptor in colon cancer cells with microsatellite instability. *Science*, *268*(5215), 1336.

Martin, S. A., Lord, C. J., & Ashworth, A. (2010). Therapeutic Targeting of the DNA Mismatch Repair Pathway. *Clinical Cancer Research*, *16*(21), 5107–5113. https://doi.org/10.1158/1078-0432.CCR-10-0821

Martincorena, I., & Campbell, P. J. (2015). Somatic mutation in cancer and normal cells. *Science*, *349*(6255), 1483–1489. https://doi.org/10.1126/science.aab4082

Martinez-Lopez, N., Athonvarangkul, D., Mishall, P., Sahu, S., & Singh, R. (2013). Autophagy proteins regulate ERK phosphorylation. *Nature Communications*, *4*(1), 2799. https://doi.org/10.1038/ncomms3799

Mateo, J., Carreira, S., Sandhu, S., Miranda, S., Mossop, H., Perez-Lopez, R., Nava Rodrigues, D., Robinson, D., Omlin, A., Tunariu, N., Boysen, G., Porta, N., Flohr, P., Gillman, A., Figueiredo, I., Paulding, C., Seed, G., Jain, S., Ralph, C., … de Bono, J. S. (2015). DNA-Repair Defects and Olaparib in Metastatic Prostate Cancer. *New England Journal of Medicine*, *373*(18), 1697–1708. https://doi.org/10.1056/NEJMoa1506859

Maya-Mendoza, A., Moudry, P., Merchut-Maya, J. M., Lee, M., Strauss, R., & Bartek, J. (2018). High speed of fork progression induces DNA replication stress and genomic instability. *Nature*, *559*(7713), 279–284. https://doi.org/10.1038/s41586-018-0261-5

Merchut-Maya, J. M., Bartek, J., & Maya-Mendoza, A. (2019). Regulation of replication fork speed: Mechanisms and impact on genomic stability. *DNA Repair*, *81*, 102654. https://doi.org/10.1016/j.dnarep.2019.102654

Mertz, T. M., Sharma, S., Chabes, A., & Shcherbakova, P. V. (2015). Colon cancer-associated mutator DNA polymerase δ variant causes expansion of dNTP pools increasing its own infidelity. *Proceedings of the National Academy of Sciences*, *112*(19), E2467–E2476. https://doi.org/10.1073/pnas.1422934112

Miyabe, I., Kunkel, T. A., & Carr, A. M. (2011). The Major Roles of DNA Polymerases Epsilon and Delta at the Eukaryotic Replication Fork Are Evolutionarily Conserved. *PLoS Genetics*, *7*(12), e1002407. https://doi.org/10.1371/journal.pgen.1002407

Nebot-Bral, L., Brandao, D., Verlingue, L., Rouleau, E., Caron, O., Despras, E., El-Dakdouki, Y., Champiat, S., Aoufouchi, S., Leary, A., Marabelle, A., Malka, D., Chaput, N., & Kannouche, P. L. (2017). Hypermutated tumours in the era of immunotherapy: The paradigm of personalised medicine. *European Journal of Cancer*, *84*, 290–303. https://doi.org/10.1016/j.ejca.2017.07.026

Nikfarjam, L., & Farzaneh, P. (2012). Prevention and Detection of Mycoplasma Contamination in Cell Culture. *Cell Journal (Yakhteh)*, *13*(4), 203–212.

Onorati, A. V., Dyczynski, M., Ojha, R., & Amaravadi, R. K. (2018). Targeting autophagy in cancer. *Cancer*, *124*(16), 3307–3318. https://doi.org/10.1002/cncr.31335

O'Rourke, J. J., Bythell-Douglas, R., Dunn, E. A., & Deans, A. J. (2019). ALT control, delete: FANCM as an anti-cancer target in Alternative Lengthening of Telomeres. *Nucleus*, *10*(1), 221–230. https://doi.org/10.1080/19491034.2019.1685246

Palles, C., Martin, L., Domingo, E., Chegwidden, L., McGuire, J., Cuthill, V., Heitzer, E., Kerr, R., Kerr, D., Kearsey, S., Clark, S. K., Tomlinson, I., Latchford, A., & The CORGI Consortium. (2021). The clinical features of polymerase proof-reading associated polyposis (PPAP) and recommendations for patient management. *Familial Cancer*. https://doi.org/10.1007/s10689-021-00256-y

Park, V. S., & Pursell, Z. F. (2019). POLE proofreading defects: Contributions to mutagenesis and cancer. *DNA Repair*, *76*, 50–59. https://doi.org/10.1016/j.dnarep.2019.02.007

Parsels, L. A., Engelke, C. G., Parsels, J., Flanagan, S. A., Zhang, Q., Tanska, D., Wahl, D. R., Canman, C. E., Lawrence, T. S., & Morgan, M. A. (2021). Combinatorial Efficacy of Olaparib with Radiation and ATR Inhibitor Requires PARP1 Protein in Homologous Recombination–Proficient Pancreatic Cancer. *Molecular Cancer Therapeutics*, *20*(2), 263–273. https://doi.org/10.1158/1535-7163.MCT-20-0365

Picard, E., Verschoor, C. P., Ma, G. W., & Pawelec, G. (2020). Relationships Between Immune Landscapes, Genetic Subtypes and Responses to Immunotherapy in Colorectal Cancer. *Frontiers in Immunology*, *11*, 369. https://doi.org/10.3389/fimmu.2020.00369

Ramsay, R. G., & Gonda, T. J. (2008). MYB function in normal and cancer cells. *Nature Reviews Cancer*, *8*(7), 523–534. https://doi.org/10.1038/nrc2439

Rane, S. G., & Reddy, E. P. (1994). JAK3: A novel JAK kinase associated with terminal differentiation of hematopoietic cells. *Oncogene*, *9*(8), 2415–2423.

Rayner, E., van Gool, I. C., Palles, C., Kearsey, S. E., Bosse, T., Tomlinson, I., & Church, D. N. (2016). A panoply of errors: Polymerase proofreading domain mutations in cancer. *Nature Reviews Cancer*, *16*(2), 71–81. https://doi.org/10.1038/nrc.2015.12

Robinson, P. S., Coorens, T. H. H., Palles, C., Mitchell, E., Abascal, F., Olafsson, S., Lee, B. C. H., Lawson, A. R. J., Lee-Six, H., Moore, L., Sanders, M. A., Hewinson, J., Martin, L., Pinna, C. M. A., Galavotti, S., Rahbari, R., Campbell, P. J., Martincorena, I., Tomlinson, I., & Stratton, M. R. (2021). Increased somatic mutation burdens in normal human cells due to defective DNA polymerases. *Nature Genetics*, *53*(10), 1434–1442. https://doi.org/10.1038/s41588-021-00930-y

Saldivar, J. C., Cortez, D., & Cimprich, K. A. (2017). The essential kinase ATR: Ensuring faithful duplication of a challenging genome. *Nature Reviews Molecular Cell Biology*, *18*(10), 622–636. https://doi.org/10.1038/nrm.2017.67

Scherr, A.-L., Mock, A., Gdynia, G., Schmitt, N., Heilig, C. E., Korell, F., Rhadakrishnan, P., Hoffmeister, P., Metzeler, K. H., Schulze-Osthoff, K., Illert, A. L., Boerries, M., Trojan, J., Waidmann, O., Falkenhorst, J., Siveke, J., Jost, P. J., Bitzer, M., Malek, N. P., … Köhler, B. C. (2020). Identification of BCL-XL as highly active survival factor and promising therapeutic target in colorectal cancer. *Cell Death & Disease*, *11*(10), 1–16. https://doi.org/10.1038/s41419-020-03092-7

Shalem, O., Sanjana, N. E., Hartenian, E., Shi, X., Scott, D. A., Mikkelsen, T. S., Heckl, D., Ebert, B. L., Root, D. E., Doench, J. G., & Zhang, F. (2014). Genome-Scale CRISPR-Cas9 Knockout Screening in Human Cells. *Science*, *343*(6166), 84–87. https://doi.org/10.1126/science.1247005

Shlien, A., Campbell, B. B., de Borja, R., Alexandrov, L. B., Merico, D., Wedge, D., Van Loo, P., Tarpey, P. S., Coupland, P., Behjati, S., Pollett, A., Lipman, T., Heidari, A., Deshmukh, S., Avitzur, N., Meier, B., Gerstung, M., Hong, Y., Merino, D. M., … Tabori, U. (2015). Combined hereditary and somatic mutations of replication error repair genes result in rapid onset of ultra-hypermutated cancers. *Nature Genetics*, *47*(3), 257–262. https://doi.org/10.1038/ng.3202

Simoneau, A., & Zou, L. (2021). An extending ATR–CHK1 circuitry: The replication stress response and beyond. *Current Opinion in Genetics & Development*, *71*, 92–98. https://doi.org/10.1016/j.gde.2021.07.003

Singh, T. R., Ali, A. M., Paramasivam, M., Pradhan, A., Wahengbam, K., Seidman, M. M., & Meetei, A. R. (2013). ATR-Dependent Phosphorylation of FANCM at Serine 1045 Is Essential for FANCM Functions. *Cancer Research*, *73*(14), 4300–4310. https://doi.org/10.1158/0008-5472.CAN-12-3976

Srivastava, S. K., Bhardwaj, A., Arora, S., Singh, S., Azim, S., Tyagi, N., Carter, J. E., Wang, B., & Singh, A. P. (2015). MYB is a novel regulator of pancreatic tumour

growth and metastasis. *British Journal of Cancer*, *113*(12), 1694–1703. https://doi.org/10.1038/bjc.2015.400

Sudbeck, E. A., Liu, X.-P., Narla, R. K., Mahajan, S., Ghosh, S., Mao, C., & Uckun, F. M. (1999). Structure-based Design of Specific Inhibitors of Janus Kinase 3 as Apoptosis-inducing Antileukemic Agents. *Clinical Cancer Research*, *5*(6), 1569–1582.

Tate, J. G., Bamford, S., Jubb, H. C., Sondka, Z., Beare, D. M., Bindal, N., Boutselakis, H., Cole, C. G., Creatore, C., Dawson, E., Fish, P., Harsha, B., Hathaway, C., Jupe, S. C., Kok, C. Y., Noble, K., Ponting, L., Ramshaw, C. C., Rye, C. E., … Forbes, S. A. (2019). COSMIC: The Catalogue Of Somatic Mutations In Cancer. *Nucleic Acids Research*, *47*(D1), D941–D947. https://doi.org/10.1093/nar/gky1015

Temko, D., Gool, I. C. V., Rayner, E., Glaire, M., Makino, S., Brown, M., Chegwidden, L., Palles, C., Depreeuw, J., Beggs, A., Stathopoulou, C., Mason, J., Baker, A.-M., Williams, M., Cerundolo, V., Rei, M., Taylor, J. C., Schuh, A., Ahmed, A., … Tomlinson, I. (2018). Somatic POLE exonuclease domain mutations are early events in sporadic endometrial and colorectal carcinogenesis, determining driver mutational landscape, clonal neoantigen burden and immune response. *The Journal of Pathology*, *245*(3), 283–296. https://doi.org/10.1002/path.5081

Thinon, E., Serwa, R. A., Broncel, M., Brannigan, J. A., Brassat, U., Wright, M. H., Heal, W. P., Wilkinson, A. J., Mann, D. J., & Tate, E. W. (2014). Global profiling of co- and post-translationally N-myristoylated proteomes in human cells. *Nature Communications*, *5*(1), 4919. https://doi.org/10.1038/ncomms5919

Tomasetti, C., Marchionni, L., Nowak, M. A., Parmigiani, G., & Vogelstein, B. (2015). Only three driver gene mutations are required for the development of lung and colorectal cancers. *Proceedings of the National Academy of Sciences*, *112*(1), 118–123. https://doi.org/10.1073/pnas.1421839112

van der Meer, D., Barthorpe, S., Yang, W., Lightfoot, H., Hall, C., Gilbert, J., Francies, H. E., & Garnett, M. J. (2019). Cell Model Passports—A hub for clinical, genetic and functional datasets of preclinical cancer models. *Nucleic Acids Research*, *47*(D1), D923–D929. https://doi.org/10.1093/nar/gky872

Vogelstein, B., Papadopoulos, N., Velculescu, V. E., Zhou, S., Diaz, L. A., & Kinzler, K. W. (2013). Cancer Genome Landscapes. *Science*, *339*(6127), 1546–1558. https://doi.org/10.1126/science.1235122

Voter, A. F., Manthei, K. A., & Keck, J. L. (2016). A High-Throughput Screening Strategy to Identify Protein-Protein Interaction Inhibitors That Block the Fanconi Anemia DNA Repair Pathway. *Journal of Biomolecular Screening*, *21*(6), 626–633. https://doi.org/10.1177/1087057116635503

Watanabe, K., Biesinger, J., Salmans, M. L., Roberts, B. S., Arthur, W. T., Cleary, M., Andersen, B., Xie, X., & Dai, X. (2014). Integrative ChIP-seq/Microarray Analysis Identifies a CTNNB1 Target Signature Enriched in Intestinal Stem Cells and Colon Cancer. *PLoS ONE*, *9*(3), e92317. https://doi.org/10.1371/journal.pone.0092317

Wheatley, S. P., & Altieri, D. C. (2019). Survivin at a glance. *Journal of Cell Science*, *132*(7), jcs223826. https://doi.org/10.1242/jcs.223826

Whitby, M. C. (2010). The FANCM family of DNA helicases/translocases. *DNA Repair*, *9*(3), 224–236. https://doi.org/10.1016/j.dnarep.2009.12.012

Williams, B. B., Wall, M., Miao, R. Y., Williams, B., Bertoncello, I., Kershaw, M. H., Mantamadiotis, T., Haber, M., Norris, M. D., Gautam, A., Darcy, P. K., & Ramsay, R. G. (2008). Induction of T cell-mediated immunity using a c-Myb DNA vaccine in a mouse model of colon cancer. *Cancer Immunology, Immunotherapy*, *57*(11), 1635–1645. https://doi.org/10.1007/s00262-008-0497-2

Xing, X., Kane, D. P., Bulock, C. R., Moore, E. A., Sharma, S., Chabes, A., & Shcherbakova, P. V. (2019). A recurrent cancer-associated substitution in DNA polymerase ε produces a hyperactive enzyme. *Nature Communications*, *10*(1), 374. https://doi.org/10.1038/s41467-018-08145-2

Yang, W., Soares, J., Greninger, P., Edelman, E. J., Lightfoot, H., Forbes, S., Bindal, N., Beare, D., Smith, J. A., Thompson, I. R., Ramaswamy, S., Futreal, P. A., Haber, D. A., Stratton, M. R., Benes, C., McDermott, U., & Garnett, M. J. (2013). Genomics of Drug Sensitivity in Cancer (GDSC): A resource for therapeutic biomarker discovery in cancer cells. *Nucleic Acids Research*, *41*(D1), D955–D961. https://doi.org/10.1093/nar/gks1111

Youle, R. J., & Strasser, A. (2008). The BCL-2 protein family: Opposing activities that mediate cell death. *Nature Reviews Molecular Cell Biology*, *9*(1), 47–59. https://doi.org/10.1038/nrm2308

Zámborszky, J., Szikriszt, B., Gervai, J. Z., Pipek, O., Póti, Á., Krzystanek, M., Ribli, D., Szalai-Gindl, J. M., Csabai, I., Szallasi, Z., Swanton, C., Richardson, A. L., & Szüts, D. (2017). Loss of BRCA1 or BRCA2 markedly increases the rate of base substitution mutagenesis and has distinct effects on genomic deletions. *Oncogene*, *36*(6), 746–755. https://doi.org/10.1038/onc.2016.243

Zeman, M. K., & Cimprich, K. A. (2014). Causes and consequences of replication stress. *Nature Cell Biology*, *16*(1), 2–9. https://doi.org/10.1038/ncb2897

Zha, J., Weiler, S., Oh, K. J., Wei, M. C., & Korsmeyer, S. J. (2000). Posttranslational N-myristoylation of BID as a molecular switch for targeting mitochondria and apoptosis. *Science (New York, N.Y.)*, *290*(5497), 1761–1765. https://doi.org/10.1126/science.290.5497.1761

Zhang, C., & Wang, Y. (2019). Metformin attenuates cells stemness and epithelial□mesenchymal transition in colorectal cancer cells by inhibiting the Wnt3a/β□catenin pathway. *Molecular Medicine Reports*, *19*(2), 1203–1209. https://doi.org/10.3892/mmr.2018.9765

Zou, L. (2007). Single- and double-stranded DNA: Building a trigger of ATR-mediated DNA damage response. *Genes & Development*, *21*(8), 879–885. https://doi.org/10.1101/gad.1550307

Zou, L., & Elledge, S. J. (2003). Sensing DNA damage through ATRIP recognition of RPA-ssDNA complexes. *Science (New York, N.Y.)*, *300*(5625), 1542–1548. https://doi.org/10.1126/science.1083430

Schwab, R.A., Blackford, A.N., and Niedzwiedz, W. (2010). ATR activation and replication fork restart are defective in FANCM-deficient cells. EMBO J *29*, 806-818.